

# **Chitosan-Based Flocculants for Mature Fine Tailings Treatment**

by

Leonardo Pennetta de Oliveira

A thesis submitted in partial fulfillment of the requirements for the degree of

Master of Science

in

Chemical Engineering

Department of Chemical and Materials Engineering

University of Alberta

## Abstract

Bitumen has been extensively extracted from oil sands through the Clark Hot Water Extraction (CHWE) process. This extraction process uses hot water and alkaline conditions to remove bitumen from oil sands ores. The tailings produced by this process are mixtures of sand, clays, residual bitumen, and salts in alkaline aqueous medium. The mining industry is currently facing increasing challenges to reduce tailings production and to reclaim the land already occupied by legacy tailing ponds.

Tailings are disposed in open pits that are called tailing ponds, which are toxic for the environment and use large areas that are difficult to reclaim. Synthetic flocculants have been used to dewater mature fine tailings (MFT), which are the denser tailings produced by the bitumen extraction process. Unfortunately, there is no current technology that can effectively dewater MFT to the desired minimum levels of 70 wt.% solids content because commercial flocculants still retain considerable amounts of water in the sediments. Mature fine tailings need to be dewatered to reduce the environmental impact caused by oil sands extraction. Polymer flocculants are commonly used to accelerate this process.

Biopolymers such as chitosan have been used to treat different types of wastewater, but not MFT. This work investigates the use of chitosan-based flocculants as an alternative to dewater MFT, due to their ability to retain less water in the sediments and their lower toxicity.

In this work, we modified chitosan, a naturally occurring biopolymer, with 3-chloro-2-hydroxypropyl trimethylammonium chloride (Chito-CTA), and also grafted polyacrylamide (PAM) to chitosan (Chito-g-PAM). We compared the dewatering performance of these two flocculants with that of a commercial cationic polyacrylamide (C-PAM). Chito-CTA and Chito-g-

PAM flocculated tailings at rates of 18.27 m/h and 20.72 m/h, respectively. The dewatering ability of Chito-CTA and Chito-g-PAM, measured in terms of capillary suction time, was below 10 seconds, whereas the value for C-PAM was 82.3 seconds at optimum dosage. The turbidity of the supernatant obtained after flocculation with Chito-CTA or Chito-g-PAM was below 10 NTU, while C-PAM produced turbid supernatants. We also studied the effect of flocculant microstructure on the specific resistance to filtration of the sediments. Chito-g-PAM produced sediments with the lowest resistance,  $2.99 \times 10^{12}$  m/kg, while C-PAM's sediments had a much higher resistance of  $40.26 \times 10^{12}$  m/kg. We also used focussed beam reflectance measurement (FBRM) technique to determine floc size evolution, floc stability, and time required to induce floc formation. Our results indicate that chitosan-based polymers may be successfully used to treat oil sands mature fine tailings.

## Preface

Chitosan was modified with varied amounts of CTA (Chito-CTA) to create positively charged quaternary ammonium groups on the polymer backbone, increasing the flocculation properties of chitosan in alkaline mediums such as MFT. Chito-CTA flocculants were compared with chitosan grafted with polyacrylamide (Chito-g-PAM) and with C-PAM, a commercial cationic flocculant. These modified polymers were then added to 5 wt.% MFT solutions to evaluate their ability to settle and dewater the suspended solids.

*Chapter 1* gives a brief history of the oil sands extraction in Canada, the composition of bitumen, the bitumen extraction process, the oil sands tailings that are produced during this extraction, and how the companies are treating these tailings. The main drawbacks of bitumen extraction processes are also defined in this chapter, as well as the technologies that are being tested to dewater the tailings such as consolidated tailings and paste technology.

*Chapter 2* reviews the previous scientific literature on MFT flocculation using polymers. This chapter describes coagulation and flocculation mechanisms involved in MFT dewatering. The natural and synthetic polymers that have been tested to treat wastewater are exemplified, including chitosan-based flocculants (Chito-CTA and Chito-g-PAM).

*Chapter 3* details the synthesis of Chito-CTA and Chito-g-PAM, and the techniques that are important to ensure that grafting reaction occur without side reactions. The methods used to characterize these polymers were Fourier-transform infrared spectroscopy (FTIR) and zeta potential. The performance of the flocculation was investigated using the following techniques: initial settling rate (ISR), capillary suction time (CST), turbidity of the supernatant, specific resistance to filtration (SRF), and focused beam reflectance measurement (FBRM).

*Chapter 4* discusses FTIR results for chitosan, CTA, PAM, Chito-CTA, and Chito-g-PAM, as well as zeta potential of polymer solutions made with Chito-CTA, Chito-g-PAM, C-PAM, and MFT. Furthermore, it presents a comparison of the 3 polymers tested, examining MFT flocculation and dewatering: ISR, CST, supernatant turbidity, SRF, and FBRM.

*Chapter 5* presents the conclusions and suggests future research work. This chapter summarizes the major findings of Chapter 4, and provides a short discussion on the results of the study. Suggestions for future studies to strengthen key knowledge gaps are also provided.

At the time of the thesis submission, several sections of this thesis were merged into a paper and submitted to the Energy and Fuels ACS Publications as L.P. de Oliveira, S. Gumfekar, F.L. Motta, and J.B.P Soares, “Dewatering of Oil Sands Tailings with Novel Chitosan-based Flocculants”.

L.P. de Oliveira was responsible for the experimentation, data analysis, and manuscript preparation. S. Gumfekar and F.L. Motta contributed with FBRM data analysis and time-to-time assistance, and J.B.P Soares was the supervisor and was also involved with the ideas and the revisions of the thesis.

The thesis is an original work by L.P. de Oliveira, with guidance and edits by S. Gumfekar, F.L. Motta, and J.B.P Soares.

## **Dedication**

After I spent several months of my life, I find myself now with the opportunity of giving thanks to others who have always been on my side on this journey and have supported me unconditionally, both at personal, professional and academic, in the accomplishment of this thesis. I begin by addressing my first thanks to Dr. Joao B.P. Soares, my supervisor, for the excellent accompaniment and commitment demonstrated during the various hours of work devoted to this master's degree. Also to Dr. Fernanda L. Motta and Sarang Gumfekar, who helped me during the whole master's degree and always did everything to pass me all their knowledge about this field.

# Table of Contents

1	Introduction.....	1
1.1	Canadian Oil Sands Reserves .....	1
1.2	Oil Sands Composition .....	2
1.3	Bitumen Extraction Process .....	3
1.4	Production of Tailings.....	5
1.5	Consolidated Tailings.....	6
1.6	Paste Technology .....	6
1.7	Problem Statement .....	6
1.8	Objectives.....	7
2	Literature Review and Theory .....	8
2.1	Oil Sands Tailings Treatment.....	8
2.1.1	Colloidal Particles.....	8
2.1.2	Coagulation.....	8
2.1.3	Flocculation .....	9
3	Materials and Methods .....	17
3.1	Materials.....	17
3.2	Synthesis of Chitosan Modified with CTA (Chito-CTA) .....	17
3.3	Synthesis of Chitosan Grafted with PAM (Chito-g-PAM) .....	17
3.4	Characterization of Flocculants and MFT.....	19
3.4.1	Fourier-Transform Infrared Spectroscopy (FTIR).....	19
3.4.2	Dean-Stark Extraction.....	19
3.4.3	Zeta Potential.....	20
3.5	Flocculant Efficiency .....	21
3.5.1	Initial Settling Rate (ISR).....	21
3.5.2	Capillary Suction Time (CST).....	21
3.5.3	Supernatant Turbidity .....	22
3.5.4	Specific Resistance to Filtration (SRF).....	22
3.6	Floc Size Measurement .....	23
4	Results and Discussion .....	24
4.1	Characterization of Chito-CTA and Chito-g-PAM .....	24

4.2	Initial Settling Rate (ISR).....	26
4.3	Capillary Suction Time (CST).....	27
4.4	Supernatant Turbidity.....	28
4.5	Specific Resistance to Filtration (SRF).....	29
4.6	Floc Formation in MFT.....	30
5	Conclusions and Future work .....	32
6	References.....	35

## List of Figures

Figure 1-1: Canadian oil sands reserves.....	2
Figure 1-2: Scheme for the Clark hot water extraction process .....	4
Figure 2-1: Chemical structures of chitin and chitosan .....	11
Figure 2-2: Chemical structure of 3-chloro-2-hydroxypropyl trimethylammonium chloride.....	15
Figure 2-3: Synthesis of chitosan grafted with 3-chloro-2-hydroxypropyl trimethylammonium chloride.....	16
Figure 3-1: Chemical reactions: (A) deacetylation of chitin to chitosan, (B) chitosan to chitosan modified with CTA (Chito-CTA), and (C) chitosan grafting with PAM (Chito-g-PAM).....	18
Figure 3-2: Schematic of a setup to measure the specific resistance of filtration of flocculated MFT .....	22
Figure 4-1: FTIR spectra of unmodified chitosan, CTA, PAM, Chito-CTA, and Chito-g-PAM .	25
Figure 4-2: Zeta potentials of the polymers synthesized in this study.....	25
Figure 4-3: Initial settling rate of MFT flocculated using: (A) Chito-CTA of varying CTA/chitosan molar ratios and dosages, and (B) different dosages of Chito-CTA (CTA/chitosan = 1304) and Chito-g-PAM.....	26
Figure 4-4: Capillary suction time of MFT flocculated using: (A) Chito-CTA of varying CTA/chitosan molar ratios and dosages, and (B) different dosages of Chito-CTA (CTA/chitosan = 1304), Chito-g-PAM, and C-PAM.....	27
Figure 4-5: Turbidity of the supernatant collected after 24 h of MFT flocculation using: (A) Chito-CTA of varying CTA/chitosan molar ratios and dosages, and (B) different dosages of Chito-CTA (CTA/Chitosan = 1304) and Chito-g-PAM. ....	28
Figure 4-6: Specific resistance to filtration of MFT after the treatment using: (A) Chito-CTA of varying CTA/chitosan molar ratios and dosages, and (B) different dosages of Chito-CTA (CTA/chitosan = 1304), Chito-g-PAM, and C-PAM.....	30
Figure 4-7: FBRM measurements for cord length and particle size distribution: (A) average floc size in MFT using 10000 ppm of Chito-CTA (CTA/chitosan = 1304), Chito-g-PAM, and C-PAM, (B) floc size distribution in MFT and MFT flocculated with 10000 ppm of Chito-CTA, Chito-g-PAM, and C-PAM.....	32

## List of Tables

Table 2-1: Properties of PAM and chitosan-based flocculants .....	13
Table 2-2: Flocculation mechanisms of chitosan-based flocculants. Reprinted with permission from Elsevier .....	14
Table 3-1: MFT composition using the Dean-Stark method.....	20
Table 3-2: MFT ion composition measured using atomic absorption spectroscopy. ....	20
Table 4-1: Dry solids cake formed of MFT flocculation using Chito-CTA of varying CTA/chitosan molar ratios and dosages, and Chito-g-PAM.....	29

# 1 Introduction

The mining of the oils sands ores in Canada is responsible for the clearing of 470 km<sup>2</sup> [1] of forest, and the creation of 220 km<sup>2</sup> of tailings ponds filled with toxic waste [2]. One of the biggest challenges facing the industry is how to dewater tailings to recover trapped water and reclaim the land occupied by tailings ponds. These components may never be decanted in a solid tank. Environmentalists and health professionals warn that this activity substantially pollutes the atmosphere, threatens the ecosystems of the area, kills fish and may be related to cases of cancer in humans [3–5].

## 1.1 Canadian Oil Sands Reserves

Oil sands exploration have a long history in Canada. In the early 1900s the soil was checked for the presence of conventional bitumen. In 1913, oil sands reservoirs were mapped in Alberta, but only on 1929 Dr. Karl Clark patented the Clark hot water extraction (CHWE) process, using water in alkaline conditions to remove bitumen from the sand [6]. In 1967, the exploitation of the oil sands reservoirs started in Canada, subsided by Great Canadian Oil Sands Limited.

Near 80 % of the total oil sands reserves in the world are in North America, and 14 % of the total reserves are found in Canada [6]. The Canadian oil sands reserves are gigantic bitumen deposits located in the Western Canada Sedimentary Basin situated in the province of Alberta. These reserves are found in three deposits: Peace River, Cold Lake, and Athabasca (Figure 1.1) [6]. Approximately 165.4 billion barrels of crude bitumen can be extracted from the oil reserves in Alberta, constituting 97% of total oil deposits in Canada [7].



**Figure 1-1:** Canadian oil sands reserves. Reprinted with permission from Elsevier [8].

The extraction and production of crude oil is around 2.5 million barrels per day. Researchers in this field expect an increase of 3.2 million barrels per day until 2020 [9].

## 1.2 Oil Sands Composition

Oil sands ores are mixtures of bitumen (10%), sand (10%), other inorganic components (75%), and water (5%) [6,10]. The American Petroleum Institute (API) created the API gravity

measurement to evaluate if petroleum is heavy or light compared to water. Bitumen is viscous, dense, and has high concentration of metals and carbon-to-hydrogen count. For this reason it is considered a heavy oil (API less than 10 degrees) [6].

Bitumen extracted from oil sands may be either sold as a mixture with a diluent (to facilitate its transportation in pipelines) or as upgraded oil with higher API. Usually, heavy oils are sold with 21.5 API and 3.3 wt.% of sulfur, and light oils are sold with 36 API and 0.015 wt.% of sulfur [6].

### **1.3 Bitumen Extraction Process**

Bitumen may be extracted from oil sands using variations of the Clark hot water extraction process (Figure 1-2) [11–13]. In this process, the oil sands ores are mixed with hot water in alkaline medium, using sodium hydroxide or sodium citrate [14].

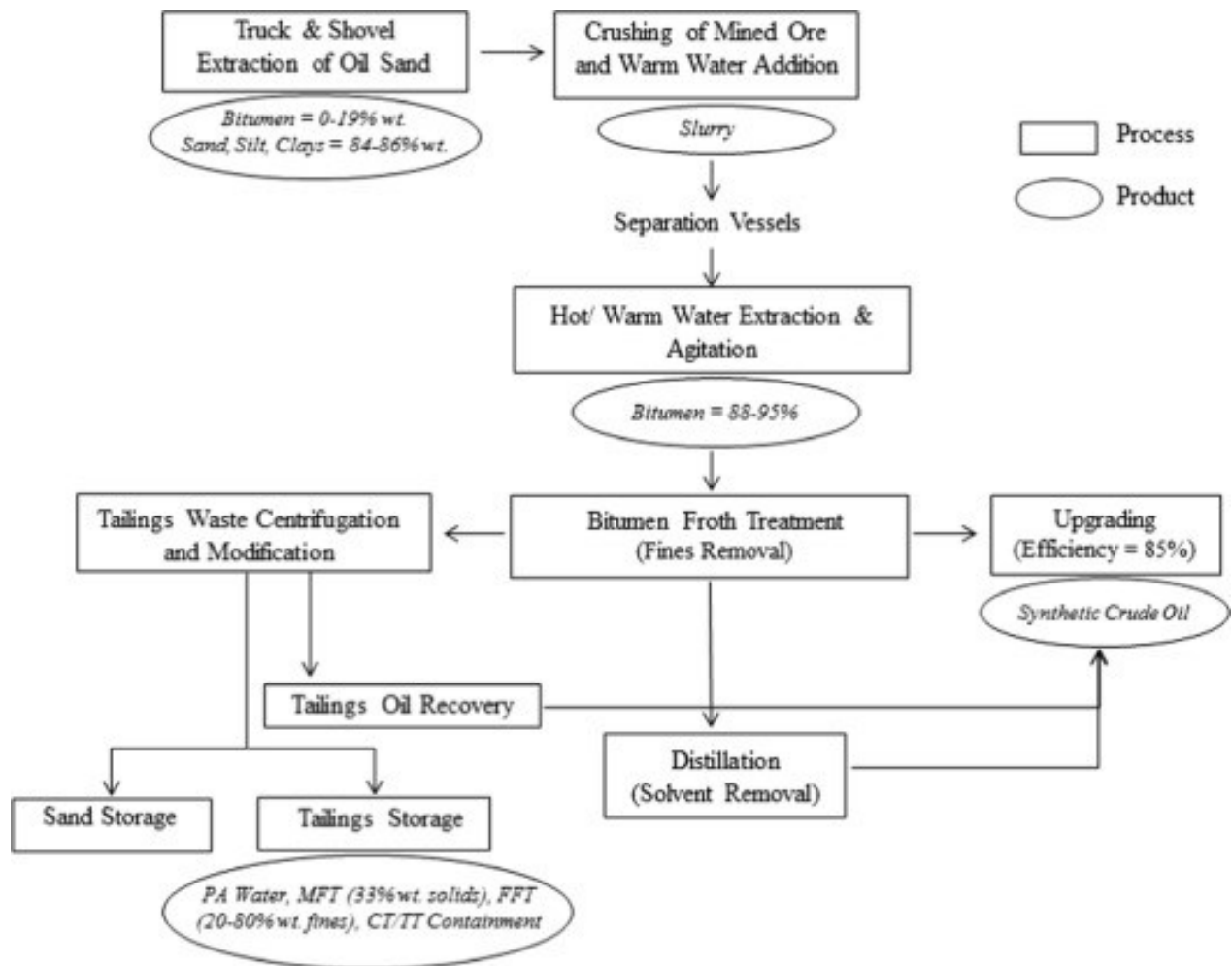


**Figure 1-2:** Scheme for the Clark hot water extraction process. Reprinted with permission from Elsevier [15].

The industrial extraction of bitumen from the oil sands ores can be made by surface mining, in-situ mining, or by a combination of both [16]. *Surface mining* is a process to extract bitumen when the deposits lie on the surface of the earth: it may range from small manual scraping on the surface of the soil to excavations that reaches hundreds of meters in depth [17]. *In-situ mining* occurs when the oil sands ores are located at such a depth that surface mining will not be able to reach the ore reserves. This type of mining requires drilling of tunnels on the ground to reach the reservoirs.

Surface mining requires more water than in situ mining (about 3 barrels of water per barrel of bitumen) [18]. To extract approximately one barrel of bitumen, the surface mining

requires on average about five times the amount of water required for in situ operations [19]. The mined components of the oil sands are shovelled, crushed, mixed with warm water to form a slurry, and transported by hydro pipeline [20]. Bitumen extraction and solvent recovery produce large quantities of process-affected water, called fluid fine tailings (FFT). As a result of the bitumen extraction process, 720 billion litres of FFT have been produced and deposited in tailing ponds [21].

#### **1.4 Production of Tailings**

Fluid fine tailings consist of water, dissolved salts, sand, clay, residual bitumen, and naphtha products [22] that are toxic for the environment. Dissolved salts can generate bivalent cations, such as  $\text{Ca}^{2+}$ , that create operational problems during the bitumen recovery process. Tailings ponds are very large containment areas where the sand present in FFT settles, form beaches, and the water and fine suspended solids form ponds [23]. After an initial stage of sedimentation and consolidation, the larger particles settle to the bottom, leaving a dense slurry layer known as mature fine tailings (MFT), which is comprised of about 70% water and 30% solids. Without any further intervention, MFT could take hundreds of years to consolidate because of the fine clay particles that are held in suspension by electrostatic interactions [24,25].

The main environmental problem that arises from the oil sands industry is contamination of water and soil due to the production of the oil sands tailings [26]. Specialists are concerned that by 2020, more than 1 billion  $\text{m}^3$  of FFT are going to be produced [6]. This situation requires efficient and sustainable processes for the treatment of tailings that have been already produced [21]. The companies that produce bitumen are trying to address this environmental problem recovering the tailing ponds and reusing the water from the extraction process, using a wide variety of methods to accelerate the tailings consolidation process. Consolidated tailings and paste technology are the most widely used methods for oil sands tailings dewatering [27].

## **1.5 Consolidated Tailings**

Consolidated Tailings (CT) use the addition of a coagulant compound to modify the surface chemistry of the MFT. Large volumes of coagulants such as gypsum or alum are mixed in the pulp. The MFT is pumped from the basin and the coagulant pulp is dosed into the MFT along with recovered silica sand. The mixture is then re-launched into the basins, where it is properly decanted as a non-segregating pulp [24]. The coagulating agents produce micro-flocs with the pulp, forming non-segregating mixtures [25]. The problem about this technique is that the high concentration of bivalent cations in the recovered water using the consolidated tailings process impedes the re-utilization of this water in the bitumen extraction process [24].

## **1.6 Paste Technology**

Paste technology (PT) is another technique for wastewater treatment due to the cost, safety of the process, and lower environmental impact. This technology uses polymer flocculants to settle the particles in suspension in the MFT and densify its sediments [24]. Differently from consolidated tailings, this process does not necessarily accumulate ions in the recycle water, but the polymer flocculants may trap a substantial amount of water in the sediments (35-40 wt.% solids) [28]. In addition, polymers are often expensive and may cause quality issues in the water recycled back from the tailings.

## **1.7 Problem Statement**

Effective dewatering of oil sands tailings is important to reduce the environmental pollution caused by oil sands operations [29]. In 2016, the Alberta Energy Regulator (AER) decreed the Directive 085, defining that the area used for the tailings ponds need to be recovered in 10 years since the deposition of the tailings [30]. The main problem is that there is no established technology to effectively dewater oil sands tailings. To solve this problem, polyacrylamide-based flocculants have been tested to flocculate MFT and recover the tailings ponds. However, these flocculants still retain a large amount of water that cannot be reclaimed from the MFT. In this work, chitosan-based flocculants were tested for MFT flocculation due to their high efficiency when flocculating

dyes from solution or textile wastewater, organic matter in pulp and paper mill wastewater, heavy metals and phenolic compounds in cardboard-mill wastewater, and inorganic suspensions in kaolinite suspension [31].

## 1.8 Objectives

This research work tested the following hypothesis: Can chitosan-based polymers effectively flocculate and dewater MFT?

The specific objectives of this study are:

- I. Synthesize a series of graft copolymers combining chitosan with 3-chloro-2-hydroxypropyl trimethylammonium chloride (CTA), where the charge density of the modified chitosan was varied to change flocculation behaviour.
- II. Synthesize a chitosan grafted with polyacrylamide (PAM).
- III. Flocculate of MFT using chitosan modified with CTA (Chito-CTA) chitosan grafted with PAM (Chito-g-PAM).
- IV. Investigate the underlying flocculating mechanism with Chito-CTA and Chito-g-PAM
- V. Compare the performance of Chito-CTA and Chito-g-PAM flocculants with a commercial cationic polymer (C-PAM).

## 2 Literature Review and Theory

### 2.1 Oil Sands Tailings Treatment

Mature fine tailings contain approximately 30 wt. % fine solids, 70 wt. % water, and 3-5 wt. % residual bitumen [32]. The main fine solids in the oil sands are clays, that are negatively charged and difficult to settle under gravity [33]. The main types of clays presented in the oil sands are kaolinite (40-70 wt. %), illite (28-45 wt. %), and montmorillonite (1-15 wt. %) [34].

#### 2.1.1 Colloidal Particles

Colloidal particles are often characterized by their sizes, surface charges, and surface functional groups. Most MFT clay particles have sizes under 45  $\mu\text{m}$ , and fines under 2  $\mu\text{m}$ .

Clays may agglomeration by coagulation or flocculation. These mechanisms destabilize colloids, possibly leading to their sedimentation [35]. This is usually achieved with the addition of chemical agents and applying mixing energy.

#### 2.1.2 Coagulation

Coagulation is a water treatment process that does not require complex equipment, is cheap, easy, and reliable [36]. The most common coagulants for MFT treatment are gypsum ( $\text{CaSO}_4$ ), sodium aluminate ( $\text{Na}_2\text{Al}_2\text{O}_3$ ), and alum ( $\text{Al}_2(\text{SO}_4)_3$ ) [37,38]. Coagulants added to water hydrolyze producing cations and anions (i.e. gypsum will hydrolyze producing  $\text{Ca}^{2+}$ ) [36]. These cations neutralize the negatively charged suspended particles, causing them to coagulate in flocs [39]. The Brownian motion and the forced convection increase the collision rate, increasing the growth of the flocs in size, and the produced flocs settle through gravity.

Coagulants, however, increase the concentration of ions in the recovered water, which may have detrimental effect in the bitumen extraction process [29]. Furthermore, flocs produced by

coagulation alone are fragile and have low shear resistance [39–41], which may cause them to break during transport in pipelines.

### **2.1.3 Flocculation**

Flocculation is an efficient method to treat tailings (and other types of wastewater) because flocculants aggregate the particles in suspension via the bridging mechanism, forming denser flocs that settle by gravity [42]. Usually, flocculants are polymers with long chains that can interact with the surface of the particles they are meant to flocculate. They adsorb onto the colloidal particles, reducing the charge of the suspended particles (charge-neutralization) and linking them into larger and heavier flocs (bridging) [40].

Synthetic polymers are the most common flocculants used in dewatering because their molecular structures can be tailored for specific applications [21,41,43]. These flocculants are usually water-soluble, and are mostly based on acrylamide and acrylic acid monomers. Examples of synthetic polymer flocculants used for MFT flocculation are: polyacrylamide, polyacrylic acid, poly(diallyl dimethyl ammonium chloride), and polyamine [44].

Synthetic flocculants are derived from petroleum derivatives [44], are non-biodegradable, and have poor shear resistance [40,45,46]. Natural polymers have been tested for wastewater treatment because they are biodegradable, non-toxic, renewable, and easily available [40,41,47]. Furthermore, natural polymers produce flocs that retain less water during the flocculation than synthetic polymers [39]. Common natural polymer flocculants include starch, chitosan, cellulose, konjac glucomanna, tamarind kernel, alginate, and guar gum [39,40,43]. They biodegrade generating by-products that do not harm the environment, but unfortunately exhibit poor flocculation performance (compared to synthetic polymers) and low storage life [39].

#### **2.1.3.1 Polymers Currently used to Flocculate MFT**

Flocculants usually promote faster flocculation rates than coagulants and make flocs that are more shear resistant [48]. The synthetic polymers that are the most widely used in MFT treatment are polyacrylamide polyacrylic acid, poly(diallyl dimethyl ammonium chloride)

(DADMAC), and polyamine [44,49]. Cationic polyelectrolytes can be used without primary coagulants, which are required for anionic or neutral polymers.

### **2.1.3.2 Polyacrylamide (PAM)**

PAM is a common flocculant for paste technology [50] because it is easy and inexpensive to be made with high molecular-weights by free radical polymerization [51]. Anionic/hydrolyzed polyacrylamide (HPAM) can adsorb onto suspended clay particles but requires the use of a coagulant, whereas cationic polyacrylamide (C-PAM) can be used alone [52]. Because PAM forms hydrogen bonds with water, it forms large flocs that holds a substantial water content [28].

### **2.1.3.3 Potential Natural Flocculants for MFT**

In recent years, different studies have been carried out on a variety of plant- and animal-derived polymers that may be used as natural flocculants. Most of them are derived from seeds, microorganisms, leaves, plant and animal tissues, barks, roots, and fruits. They are biodegradable and safe for human health. These natural flocculants are often polysaccharides and proteins, which are an alternative source with great potential not yet sufficiently exploited. The most common polysaccharides that have been tested for waste water flocculation are cellulose, starch, and chitosan [53], being the latter the object of study of this work.

### **2.1.3.4 Chitin**

After cellulose, chitin is the second most abundant natural polymer in the world [54]. It is found in fungi, mollusks, insects, and crustaceans. Crustaceans are extensively used for human consumption, but their heads and the tails, having a high chitin content, are discarded. In 2011, the Food and Agriculture Organization of the United Nations estimated that 5.9 Mt of crustaceans are consumed per year [55].

Chitin is a polysaccharide containing of  $\beta$ -1,4-N-acetylglucosamine and, like cellulose, it is neutral, linear, and stable. Usually, chitin is insoluble in most solvents, preventing it from being used for flocculation [56,57].

Chitin can be deacetylated (removal of one acetyl group) by N-deacetylation to produce chitosan, which is composed of glucosamine and N-acetylglucosamine units [58]. When the percentage of N-acetyl-glucosamine is more than 60 mol%, the product is called chitin, but if the amount of N-glucosamine units is higher than 60 mol%, it is named chitosan (Figure 2-1) [59].

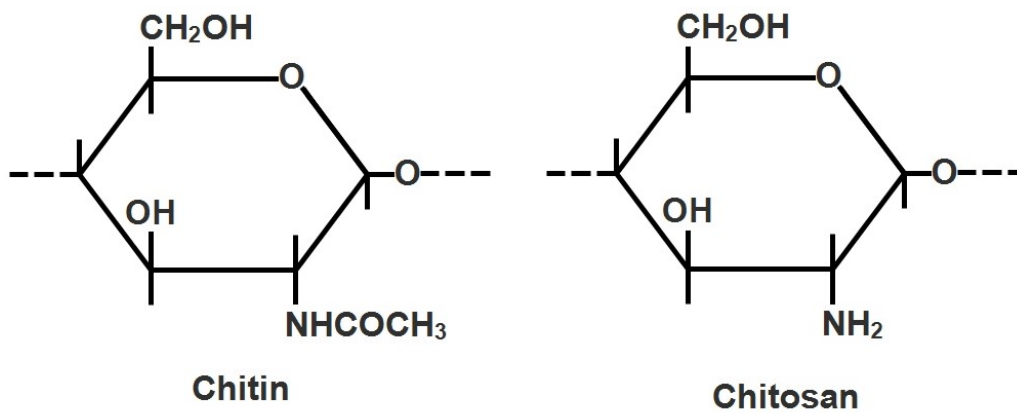


**Figure 2-1:** Chemical structures of chitin and chitosan [60].

### 2.1.3.5 Chitosan

Chitosan can be made by N-deacetylation of crustacean shells when they are exposed at high temperatures and alkaline mediums [55]. Chitosan is one of the most promising biopolymers for extensive application because it is cationic [44]. It is a linear hydrophilic amino-polysaccharide with a rigid structure containing both glucosamine and acetylglucosamine units [61]. It is insoluble in either water or organic solvents, but soluble in dilute organic acids such as acetic acid and formic acid, as well as in inorganic acids (with the remarkable exception of sulphuric acid) where the free amino groups are protonated, making it fully soluble [62,63]. At acidic pH (below  $\sim$ pH 4), chitosan becomes a soluble cationic polymer with high charge density [64]. Thus, treatment of wastewater with chitosan dissolved in acids produces protonated amine groups along the chain and

this facilitates electrostatic interactions between polymer chains and the negatively charged contaminants (metal anions, dyes, organic compounds, etc.)

Chitosan possesses characteristics such as high cationic charge density (amino groups) and long polymer chains that make it an effective coagulant and/or flocculant for the removal of contaminants in suspended dissolved in water [65]. As the active amino groups ( $\text{NH}_2$ ) in the chitosan molecule can be protonated with  $\text{H}^+$  in water into a cationic polyelectrolyte, the molecule has characteristics of static attraction and adsorption [31]. Besides, chitosan can also flocculate particles into bigger flocs which can settle by gravity. Therefore, the development of chitosan-based materials as useful flocculants is an expanding field in the area of water and wastewater treatment. Numerous works have demonstrated its outstanding coagulation and flocculation properties of dye molecules in textile wastewater, organic compounds in pulp and paper mill wastewater, heavy metals and phenolic compounds in cardboard-mill wastewater, and kaolinite suspensions [44].

Chitosan-based polymers dewater kaolin suspensions better than PAM flocculants [11]. These suspensions are sometimes used as models for MFT. In addition flocculants based on chitosan can be recovered and recycled by adding alkali solution, filtered, and reused without drying. Recyclability of chitosan is more efficient than PAM-based flocculants with an efficiency up to 98 % recovery [66], although this may not be applicable for MFT applications because of the high solids content and presence of residual bitumen.

Table 2-1 lists the main advantages of chitosan-based flocculants compared PAM-based flocculants.

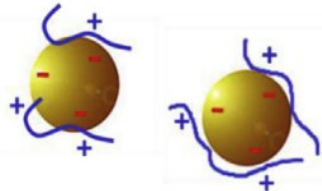
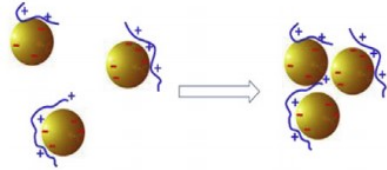
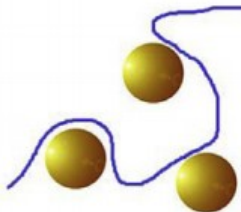
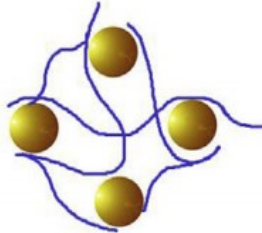
**Table 2-1:** Properties of PAM and chitosan-based flocculants [44].

<b>Properties</b>	<b>PAM-based flocculants</b>	<b>Chitosan-based flocculants</b>
<b>Dewatering efficiency*</b>	Low efficiency (Turbidity: 6.8–25 NTU)	High efficiency (Turbidity: 1.1–10 NTU)
<b>Renewability</b>	Made of non-renewable fossil fuels	Extracted from crustaceous shells
<b>Recyclability</b>	Non-recyclable	Efficiency up to 98% recovery
<b>Biodegradability</b>	Non-biodegradable	Biodegradable
<b>Flocculation mechanism</b>	Bridging	Bridging and neutralization mechanism

\*Note: The results for dewatering efficiency are based on pulp and paper mill wastewater.

The performance of chitosan can be improved when it is combined with other materials to produce composites that can reinforce its functional properties [54]. The amino ( $-NH_2$ ) and hydroxyl ( $-OH$ ) groups present on the chitosan backbone can be used as grafting sites. The grafting copolymerization of chitosan with a variety of cationic monomers using redox initiators has been reported in literature [67]. Chitosan-based flocculants have been synthesized and tested with wastewater contaminated with dissolved and undissolved inorganic, organic, and biological contaminants, including suspended solids, heavy metals, humic acid, dyes, algae, and bacteria [68]. Chitosan-based flocculants have four different mechanisms to flocculate solid particles: simple charge neutralization, charge patching, bridging, and sweeping (Table 2-2) [41].

**Table 2-2:** Flocculation mechanisms of chitosan-based flocculants. Reprinted with permission from Elsevier [54].

Mechanism	Description	Illustration
<b>Simple charge neutralization</b>	Efficient reduction of the thickness of the electric double layer and full charge neutralization.	
<b>Charge patching</b>	Unevenly distributed surface charges are incompletely neutralized.	
<b>Bridging</b>	Adsorption and connection of the primary flocs on soluble linear large molecular weight flocculants.	
<b>Sweeping</b>	Enmeshing and entrapping of small colloidal pollutants by large flocs or polymeric precipitates.	

### 2.1.3.6 Quaternized Carboxymethyl Chitosan

Chemically-modified chitosan derivatives have been studied recently. One purpose of these chemical modifications, which include saccharization, alkylation, acylation, quaternization and metallization, is to improve solubility in water [69]. Among amphoteric chitosan-based flocculants, the simplest one is carboxymethyl chitosan (CMC) [70]. The solubility of chitosan can be enhanced by the carboxymethylation of chitosan with monochloroacetic acid in the presence of sodium hydroxide (NaOH) [71]. Carboxymethylation increases the viscosity, improves moisture retention, and expands the flocculation properties of these polymers. However,

CMC is not the best option to flocculate Cr(VI) and some negative colloidal particles in wastewater, since the carboxymethyl groups ( $-\text{CH}_2\text{COOH}$ ) added to chitosan only increase the negative charges in the molecule, not affecting its positive charges [72].

Usually, quaternary modification can be a good method to add positive charges in polymer flocculants. Quaternary chitosan is prepared by adding quaternary ammonium groups onto the chitosan backbone [73]. The amino group presented in chitosan contains reactive hydrogen atoms that can react with ammonium groups [69]. Instead of adding carboxymethyl groups, quaternary ammonium groups ( $-\text{CH}_2\text{CH}(\text{OH})\text{CH}_2\text{N}^+(\text{CH}_3)_3\text{Cl}^-$ ) can be supplemented into the molecular chain with 3-chloro-2-hydroxypropyl trimethylammonium chloride (CTA) as grafting agent [72]. CTA is a grafting agent that is used in industry due to the positive and negative charges in its structure (Figure 2-2), and its low toxicity [43]. The main characteristic of quaternary ammonium groups is that they do not lose their positive charges in different media [74].

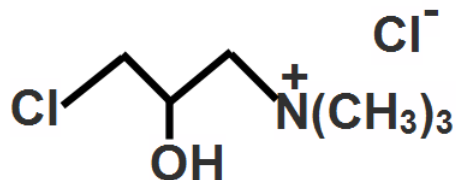


**Figure 2-2:** Chemical structure of 3-chloro-2-hydroxypropyl trimethylammonium chloride.

CTA can be added to the chitosan backbone in the presence of NaOH to produce Chito-CTA (Figure 2-3). This reaction increases the solubility of chitosan in more alkaline mediums improves the flocculation properties, but it is still insoluble at higher pH values [43]. Chitosan contains primary hydroxyl groups, secondary hydroxyl groups, and amino groups that can react with CTA, producing, respectively, N-carboxymethyl chitosan (N-CMCs), N,O-carboxymethyl chitosan (N,O-CMCs), and O-carboxymethyl chitosan (O-CMCs). The later is favored when the quaternary modifications happens in aqueous solution with sodium hydroxide at low temperatures [75].

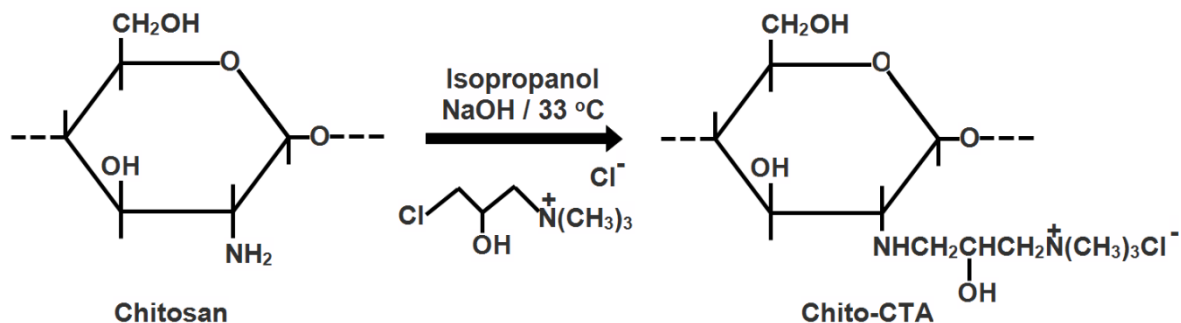


**Figure 2-3:** Synthesis of chitosan grafted with 3-chloro-2-hydroxypropyl trimethylammonium chloride.

### 2.1.3.7 Chitosan-Graft-Polyacrylamide

To combine the properties of synthetic and natural polymers, chemically modified polysaccharides are being developed and tested. Polysaccharide backbones can be polymerized with acrylamide to tune the properties of the flocculant, forming graft copolymers [52] that are more easily biodegraded. The graft macromolecule chains are also stronger, increasing the stability of the polymer [52,76].

Even though chitosan-based flocculants increase the solubility of chitosan in water, their applicability is limited because of their lower molecular weight and shorter storage life. It is known that polyacrylamide is efficient for wastewater treatment [77] and can be copolymerized with polysaccharides. The graft polymerization between chitosan and polyacrylamide can combine the advantages of both polymers, increasing the molecular-weight and reducing the biodegradability of the flocculants [51]. Chitosan can be polymerized with PAM to produce chitosan-graft-polyacrylamide (Chito-g-PAM).

# 3 Materials and Methods

## 3.1 Materials

Chitosan (75 wt.% deacetylation, molecular weight 310,000-375,000 Da), 3-chloro-2-hydroxypropyl trimethylammonium chloride (CTA) (60 wt. % solution in H<sub>2</sub>O), acrylamide, ceric ammonium nitrate (CAN), acetone (99.9 %), and sodium hydroxide (NaOH) were purchased from Sigma-Aldrich. The reference cationic polyacrylamide (C-PAM) had a molecular weight of approximately 10,000,000 Da and 20 % cationic charge density. We selected a cationic PAM as reference material since Chito-CTA is also a cationic polymer. Isopropanol (99.9 %) and hydrochloric acid (HCl) were purchased from Fisher Scientific. Imperial Oil (Fort McMurray, AB, Canada) provided the MFT samples used in our investigation.

## 3.2 Synthesis of Chitosan Modified with CTA (Chito-CTA)

The chitosan used in study is made by the deacetylation of chitin (Figure 3-1.A). We dispersed chitosan in distilled water (2.8 g/L), heated it to 33 °C for 30 min, and added 15 mmol NaOH (1 mol/L stock solution). After mixing the suspension for 15 min, we added an aqueous solution of CTA (60 wt. % solution in H<sub>2</sub>O) and maintained the temperature at 33 °C for 18 h. We stopped the reaction by adding HCl until the pH of the mixture dropped below 7. CTA caused the quaternization of chitosan, improving its solubility in water. We varied the degree of quaternization by changing the molar ratio CTA/chitosan from 163 to 1304. We precipitated and washed the reaction mixture in excess isopropanol 3 times to remove unreacted CTA. Finally, we dried the washed Chito-CTA under vacuum at 40 °C for 24 h. The scheme we followed to modify chitosan with CTA is shown in Figure 3-1.B.

## 3.3 Synthesis of Chitosan Grafted with PAM (Chito-g-PAM)

We dissolved chitosan in 1 % acetic acid aqueous solution (0.0046 g/mL) under continuous nitrogen flow for 30 min. Next, we added CAN initiator (0.0015 g/mL) to the reaction mixture

under continued stirring for 15 min. Further, we added 0.15 g acrylamide dissolved in 50 mL water dropwise to the reaction mixture. We continued the polymerization of acrylamide in presence of chitosan for 3 h at room temperature. We precipitated final product the in excess acetone and dried it under vacuum at 40 °C for 48 h. The is procedure is depicted in Figure 3-1.C. Two mechanisms for the reaction were found in the literature and are illustrated in the Figure 3-1.C [78,79].

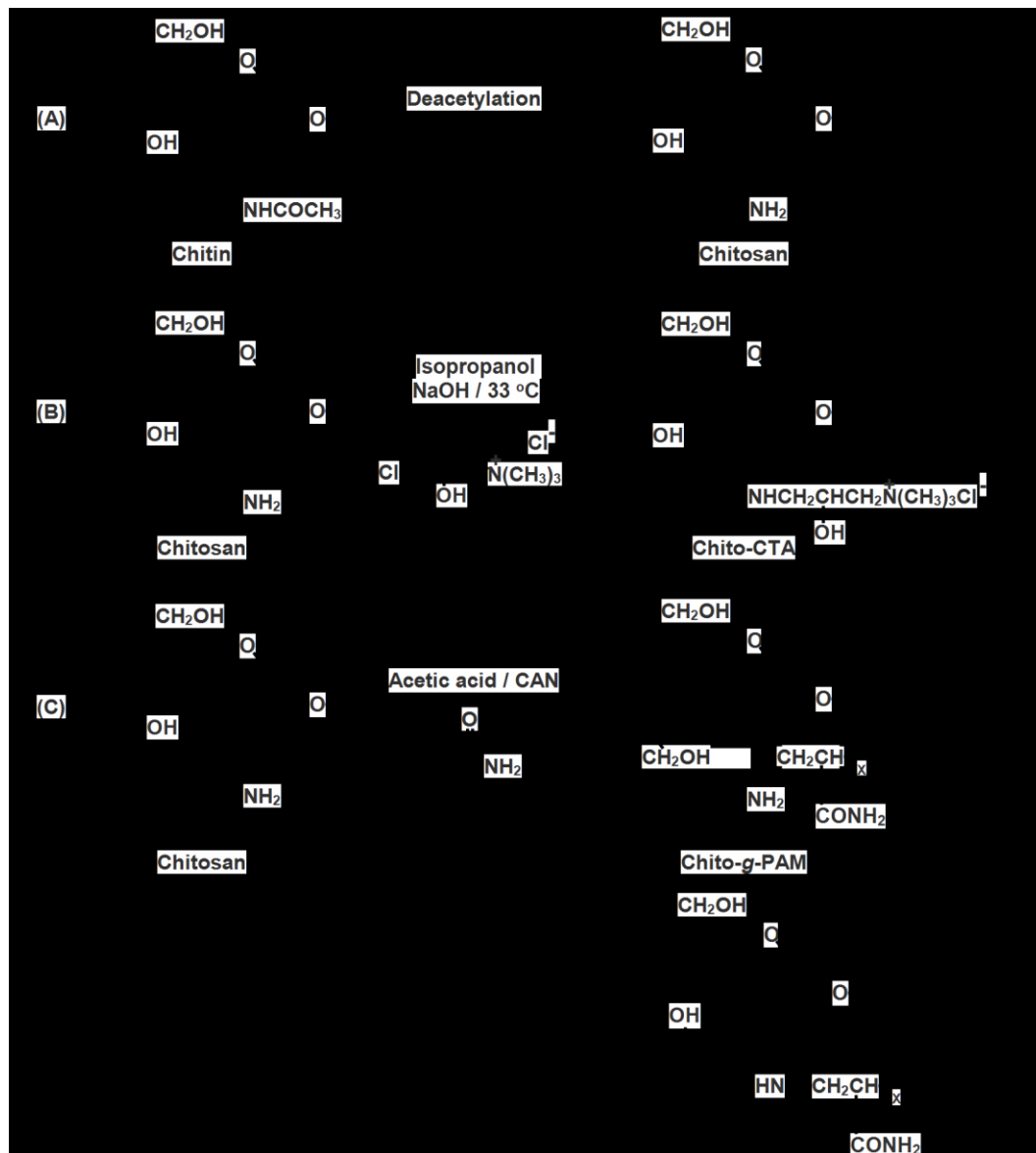


**Figure 3-1:** Chemical reactions: (A) deacetylation of chitin to chitosan, (B) chitosan to chitosan modified with CTA (Chito-CTA), and (C) chitosan grafting with PAM (Chito-g-PAM).

## **3.4 Characterization of Flocculants and MFT**

### **3.4.1 Fourier-Transform Infrared Spectroscopy (FTIR)**

FTIR is a characterization technique that measures the interaction of the functional groups in the structure of chemical compounds with the infrared light. It is a fast analysis with high reproducibility.[80] The detector produces spectra of the samples with frequencies varying between 4000 to 400  $\text{cm}^{-1}$  [81]. The samples tested using FTIR can be small and in different states (solid, liquid, or gas). FTIR is a helpful tool to analyze copolymers because these macromolecule may be considered simple mixtures of their comonomers [82,83].

The FTIR spectra of polymers modified with grafting agents shows new peaks derived from the functional groups added to the structure. The intensity and the dispersion of the peaks depend on the degree of grafting. FTIR of chitosan, CTA, PAM, Chito-CTA (CTA/chitosan molar ratio = 1630), and Chito-g-PAM, measured in an Agilent Technologies Cary 600 Series FTIR spectrometer in the range of 400-4000  $\text{cm}^{-1}$ , will be explained in Chapter 4 (Figure 4-1).

### **3.4.2 Dean-Stark Extraction**

The Dean–Stark extraction was used to measure the amount of residual bitumen, solids, and water in the MFT sample. To perform a Dean-Stark analysis, one needs a round bottom flask, a reflux condenser, and a trap. A mass of 120 g of MFT is placed in the trap, 300 mL of toluene is poured into the round bottom flask, and the apparatus is heated up to 200 °C. The liquids separate in two layers: toluene (top layer) and water (bottom layer). The toluene that was condensed produces a reflux that mixes with the MFT sample and dissolves the organic components in MFT. When the water level stabilizes, water is drained from the trap and its mass is measured. Toluene is evaporated from the toluene-bitumen mixture and the solids are weighted.

We used the Dean–Stark extraction method to determine the amount of solids, water, and bitumen in the MFT sample (Table 3-1). Atomic absorption spectroscopy (AAS) was used to quantify the concentration of major ions in the MFT sample (Table 3-2). The MFT used to perform the flocculants tests in this work was the same characterized by Thompson et al. [84].

**Table 3-1:** MFT composition using the Dean-Stark method.

<b>Compound</b>	<b>Weight %</b>
<b>Water</b>	62.7
<b>Solids</b>	32.3
<b>Bitumen</b>	4.2

**Table 3-2:** MFT ion composition measured using atomic absorption spectroscopy.

<b>Ion</b>	<b>Quantity (ppm)</b>
<b>Na<sup>+</sup></b>	251.6
<b>K<sup>+</sup></b>	17.3
<b>Ca<sup>2+</sup></b>	25.6
<b>Mg<sup>2+</sup></b>	12.4

### 3.4.3 Zeta Potential

Zeta potential measures the electrophoretic mobility of particles in suspension. It is a good indicator of interactions between particles, and of suspension stability. The stability of colloidal suspensions is determined by van der Waals attractive forces and electrical double layer repulsive forces that exist among suspended particles. MFT contains clays that are usually negatively charged, and dissolved salts that are positively charged. These negatively-charged particles repel each other, producing a stable suspension. Zeta potential was measured to determine how chitosan-based polymers interacted with MFT. We measured the zeta potential of the polymer dispersions synthesized in this study using a Zetasizer Nano unit (Malvern). The solution concentration was maintained at 1 mg/mL in deionized water at pH 7.

### **3.5 Flocculant Efficiency**

The efficiency of flocculant can be measured by different performance indicators, such as initial settling rate (ISR), capillary suction time (CST), supernatant turbidity, specific resistance to filtration (SRF), and focused beam reflectance measurement (FBRM) [44]. Chito-CTA, Chito-g-PAM, and C-PAM were used to coagulate/flocculate MFT slurries diluted with deionized water to 5 wt%. For Chito-CTA, coagulation is a more likely mechanism, although flocculation may also happen. Flocculation experiments were carried out with 150 mL of a 5 wt. % solids suspension prepared by diluting MFT with deionized water in a 250-mL baffled beaker. We dosed the diluted MFT with 3000, 5000, 7000, and 10000 ppm of flocculant (on a weight basis relative to the weight of solids in the MFT). The MFT suspension was mixed in two stages: 1) at 600 rpm using a 45 degree Pitch Blade Turbine (PBT) - 4 blades impeller (4.8 cm diameter) for 1 min to ensure uniform solids dispersion, and 2) at 300 rpm for 1 min, while the desired amount of flocculant was added into the MFT suspension. After the second mixing step, we immediately transferred the mixture to a 100 mL graduated cylinder, and recorded the mudline position (solid-liquid interface) for 1 h.

#### **3.5.1 Initial Settling Rate (ISR)**

ISR is a technique that uses a 100 mL graduated cylinder and a stopwatch. The MFT/flocculant suspensions were placed in 100 mL graduate cylinders and the cylinders were sealed. The slurry was allowed to settle, forming a descending solid–liquid interface that could be measured over time [85]. The ISR of the suspension was calculated from the slope of the straight-line portion of the plot of the interface height versus the settling time.

#### **3.5.2 Capillary Suction Time (CST)**

CST is a technique that measures how fast the settled flocs dewater [86]. CST determines how fast sediments can be dewatered, by measuring the time taken by water to travel a certain radial distance over filter paper [87]. Shorter times indicate better dewaterability. The analyses were always performed in three replicates, to calculate average CSTs and standard deviation. CST

of the suspension after flocculation was measured using a Triton Electronics 319 multi-purpose CST apparatus using a standard Triton filter paper (7 cm × 9 cm).

### 3.5.3 Supernatant Turbidity

Supernatant turbidity measures how much solid is present in the supernatant after flocculation. Since this water needs to be recycled to the bitumen extraction process, low turbidity is preferable, otherwise fine particles will accumulate in the system over time. At the end of the settling period, the supernatant suspension was collected using a pipette and its turbidity was measured using a Hach 2100AN turbidimeter [85]. The results were expressed in nephelometric turbidity unit, NTU.

### 3.5.4 Specific Resistance to Filtration (SRF)

The pressure filtration was performed in a pressure filtration unit (Figure 3-2). The pressure during the filtration remained constant during the whole process (30 psi).

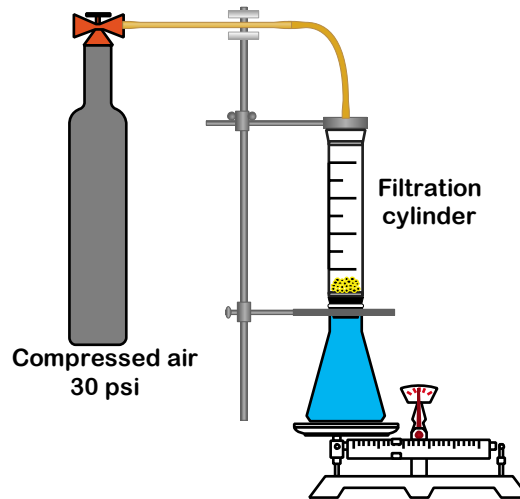


**Figure 3-2:** Schematic of a setup to measure  $t$  specific resistance of filtration of flocculated MFT.

The SRF of MFT after flocculation was calculated using Equation (3.1) [88]:

$$\text{SRF} = \frac{2PA^2}{\mu\omega} b \quad (3.1)$$

where,  $P$  is the pressure (Pa),  $A$  is the filter area ( $\text{m}^2$ ),  $b$  is the slope calculated from the plot of  $t/V$  against  $V$ ,  $V$  is the volume of filtrate ( $\text{m}^3$ ),  $t$  is the filtration time (s),  $\mu$  is the viscosity of filtrate ( $\text{Pa}\cdot\text{s}$ ), and  $\omega$  is the mass of solids cake formed per unit filtrate volume ( $\text{kg}/\text{m}^3$ ).

The pressure filtration test was conducted using a stainless-steel cylinder (47 mm diameter) with a capacity of approximately 200 mL (Advanted, KST-47). The filter paper, Whatman no. 4 (35 mm diameter), was placed at the bottom of the cylinder. The mixture of MFT and flocculant was fed into the cylinder and a compressed air source was connected to the top of the cylinder. The regulator was adjusted to pressurize the system up to 30 psi. After the system was pressurized, water started to drain from the bottom of the system and was collected in a beaker placed on top of a balance (Ohaus, AX223). The balance was connected to a control panel that recorded the weight of the filtrate every 10 s. Plots for time versus filtrate volume were obtained from these measurements and used to calculate SRF.

### 3.6 Floc Size Measurement

We used focused beam reflectance measurement instrument (FBRM G400, Mettler-Toledo, USA) to measure the floc size evolution in real time before and after flocculant addition [89–91]. The FBRM probe consists of a fast-rotating laser beam, which is immersed in a beaker containing the MFT/flocculant suspension. The incident laser beam is reflected by the suspended solids, and is captured by the FBRM probe. The multiplication of the beam reflectance speed and the duration of the reflected signal gives the *chord length*, which is a measurement of floc/particle size. We also obtained floc size distributions before and after addition of the flocculants. These experiments were carried out with only 7000 ppm of Chito-CTA, Chito-g-PAM, and C-PAM.

## 4 Results and Discussion

### 4.1 Characterization of Chito-CTA and Chito-g-PAM

The FTIR spectra of unmodified chitosan, CTA, PAM, Chito-CTA, and Chito-g-PAM are compared in Figure 4-1. The spectrum for chitosan shows the characteristic frequencies for O-H stretch at  $3000\text{ cm}^{-1}$ , N-H bend at  $1400\text{ cm}^{-1}$ , and bridge-O stretch at  $1100\text{ cm}^{-1}$  [47]. To confirm the modification of chitosan with CTA, we first analyzed CTA by FTIR, showing the signature frequency for the methyl group of the quaternary ammonium group at  $1488\text{ cm}^{-1}$ . In Chito-CTA, this peak position shifts to  $1371\text{ cm}^{-1}$ . Two functional groups on chitosan, amine and hydroxyl, may react with CTA. The spectrum of Chito-CTA shows that hydroxyl groups are present, implying that CTA reacted with amine groups. PAM can be identified by its characteristic amide C=O peak at  $1670\text{ cm}^{-1}$ , which is also present in the spectrum of Chito-g-PAM. The intensity of the hydroxyl peak in the spectrum of Chito-g-PAM is low, implying that PAM was grafted to chitosan through hydroxyl groups.

We also confirmed the modification of chitosan by measuring its zeta potential at pH 7. As expected, increasing the molar ratio of CTA to chitosan increased the zeta potential of the polymer dispersion, as shown in Figure 4-2. Chito-g-PAM and commercial C-PAM had zeta potentials of  $39.5 \pm 4.07$  and  $37.3 \pm 3.12$  mV, respectively.

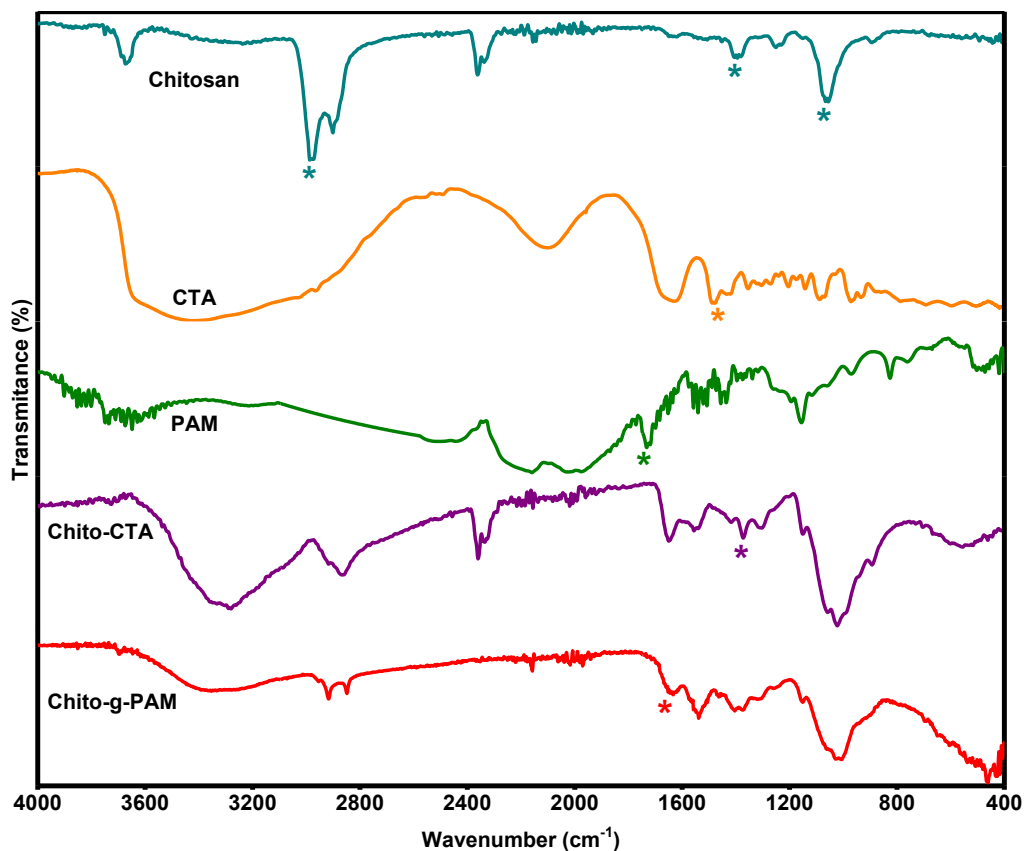


Figure 4-1: FTIR spectra of unmodified chitosan, CTA, PAM, Chito-CTA, and Chito-g-PAM.

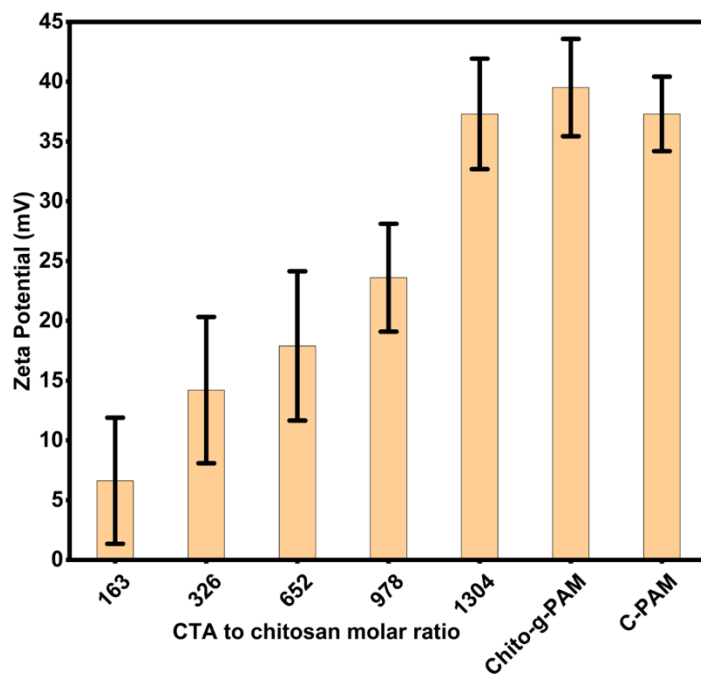
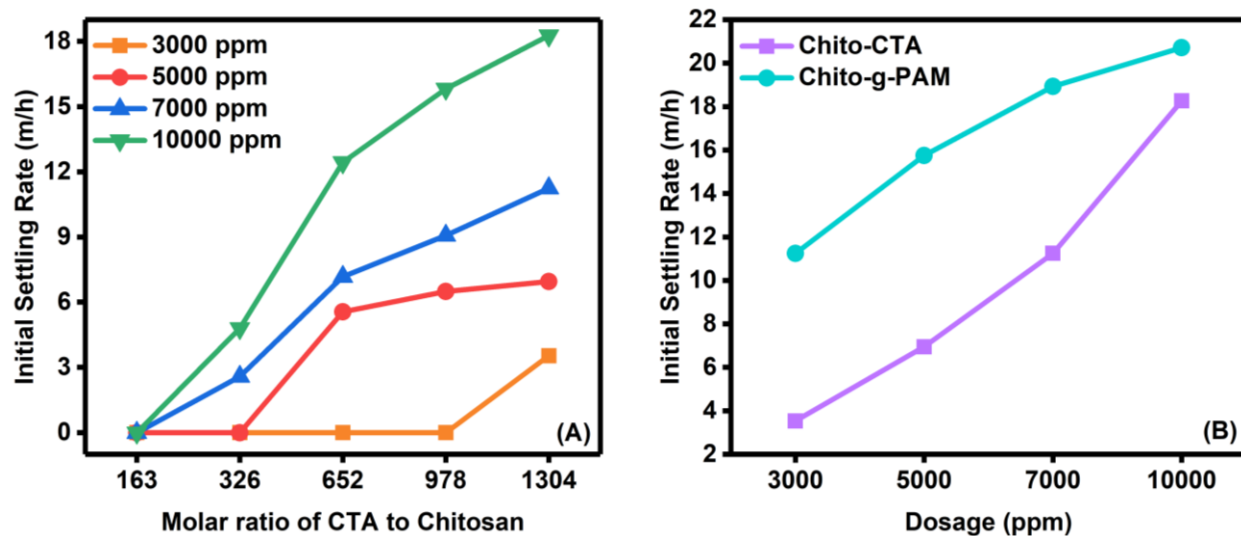


Figure 4-2: Zeta potentials of the polymers synthesized in this study.

## 4.2 Initial Settling Rate (ISR)

We flocculated 5 wt% MFT with Chito-CTA having varying CTA/chitosan molar ratios, Chito-g-PAM, and commercial C-PAM. Figure 4-3.A and 4-3.B compare these results. Coagulation experiments with Chito-CTA were carried out with dosages varying from 3000 to 10000 ppm. At 3000 ppm, MFT settled significantly only the CTA/chitosan molar ratio was 1304. As we increased the dosage up to 10000 ppm, MFT settled at lower CTA/chitosan ratios, indicating that the sufficient cation density required to induce the solid-liquid separation in MFT was achieved. When Chito-CTA had lower cation charge density, higher dosages were required to initiate the flocculation. At 10000 ppm, ISR increased up to 18 m/h, due to the increase in electrostatic interactions between negatively-charged MFT clays and positively-charged polymer backbones [92]. Figure 4-3.B compares the effect of different dosages of Chito-CTA (CTA/chitosan = 1304) and Chito-g-PAM on ISR. Chito-g-PAM always outperformed Chito-CTA, while C-PAM did not effectively flocculate the MFT sample. The ISR for C-PAM is not shown in Figure 4-3 because we could not clearly distinguish the solid-liquid interface, which is needed to calculate ISR.



**Figure 4-3:** Initial settling rate of MFT flocculated using: (A) Chito-CTA of varying CTA/chitosan molar ratios and dosages, and (B) different dosages of Chito-CTA (CTA/chitosan = 1304) and Chito-g-PAM.

### 4.3 Capillary Suction Time (CST)

CST is a measure of the dewaterability of sludges. It is often used to quantify the performance of MFT flocculants [32]. A lower CST correlates with higher dewaterability. Figure 4-4.A shows the effect of CTA/chitosan molar ratio and polymer dosage on CST. Pure MFT has a CST higher than 300 s, but CST decreased with increasing dosage of Chito-CTA at any given CTA/chitosan molar ratio. In addition, CST decreased when the CTA/chitosan molar ratio increased from 163 to 1304. Typically, CST values of less than 20 s are acceptable in the oil sands industry. We speculate that Chito-CTA formed dense flocs that were nearly closed (low porosity), which reduced the diffusion of water into the flocs and caused the CST to decrease with increasing polymer dosage. Figure 4-4.B compares the CST for MFT sediments produced by adding Chito-CTA (CTA/chitosan = 1304), Chito-g-PAM, and C-PAM at different dosages. The commercial C-PAM did not significantly reduce the CST even at the highest dosage, while Chito-CTA and Chito-g-PAM reduced the CST to industrially acceptable limits. At lower dosages of 3000 and 5000 ppm, Chito-g-PAM dewatered MFT faster than Chito-CTA, likely because of its longer PAM branches.

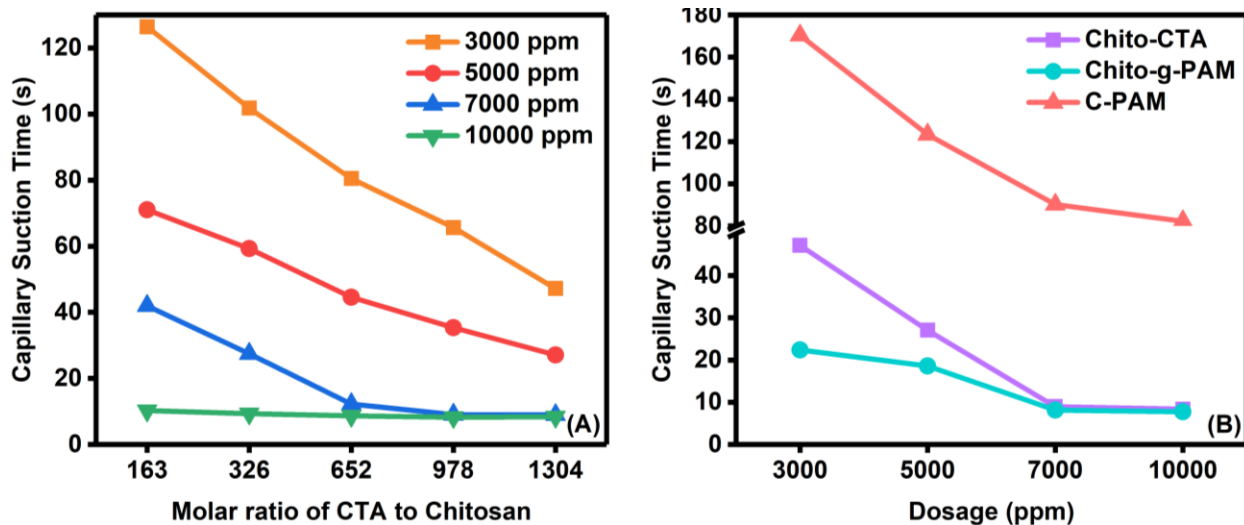


**Figure 4-4:** Capillary suction time of MFT flocculated using: (A) Chito-CTA of varying CTA/chitosan molar ratios and dosages, and (B) different dosages of Chito-CTA (CTA/chitosan = 1304), Chito-g-PAM, and C-PAM.

## 4.4 Supernatant Turbidity

The quality of the water recovered after the flocculation was measured by its turbidity. The presence of electrostatically stable particles in the supernatant increases its turbidity. Figure 4-5.A shows the turbidity of the supernatant collected after 24 h Chito-CTA was added to MFT. In general, the supernatant turbidity decreased with increasing polymer dosage, because either more flocs were formed, or flocs grew larger when more polymer was added to the suspension. Other researchers reported similar observations for MFT flocculation [87]. The supernatant turbidity also decreased significantly for higher CTA/chitosan molar ratios. The effect of CTA/chitosan molar ratio may be explained in terms of increased charge neutralization of fine particles in the supernatant due to the increased cation density at higher CTA/chitosan molar ratios.

Figure 4-5.B compares supernatant turbidities measured using Chito-CTA (CTA/Chitosan = 1304), Chito-g-PAM, and C-PAM. The commercial C-PAM produced very turbid supernatant, while Chito-g-PAM led to the clearest supernatants for all dosages. Chito-g-PAM seemed to be the polymer best suited to capture the majority of the fine particles, which are otherwise difficult to flocculate/coagulate using linear polymers. Chito-CTA produced acceptable supernatants only at 7000 and 10000 ppm dosages.

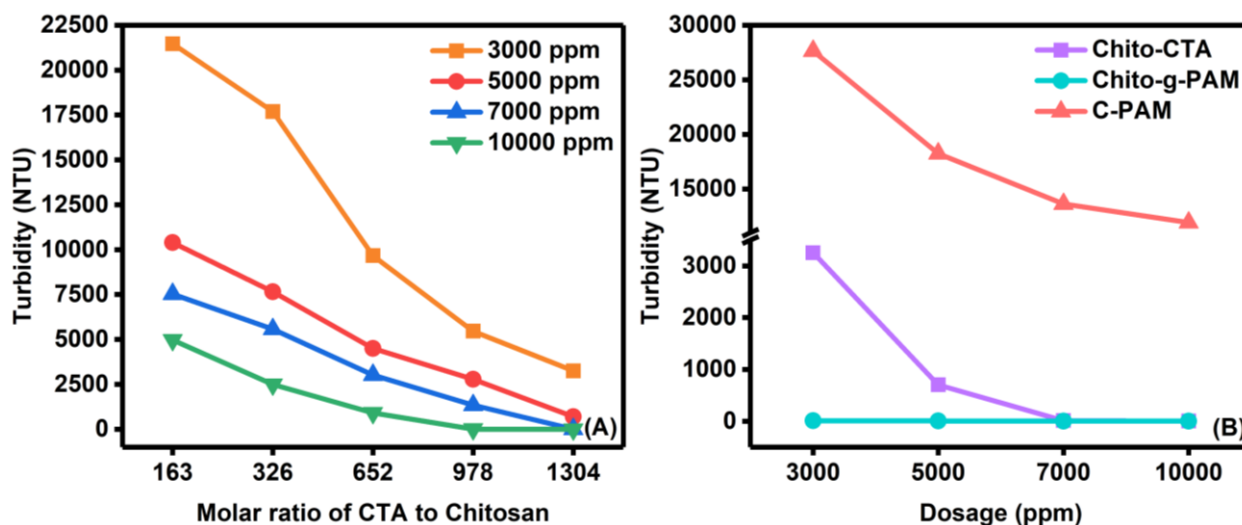


**Figure 4-5:** Turbidity of the supernatant collected after 24 h of MFT flocculation using: (A) Chito-CTA of varying CTA/chitosan molar ratios and dosages, and (B) different dosages of Chito-CTA (CTA/Chitosan = 1304) and Chito-g-PAM.

## 4.5 Specific Resistance to Filtration (SRF)

The SRF, calculated with Equation (3.1), quantifies the filterability of MFT after its treatment with a flocculant. The dry solids cake formed can be seen in Table 4-1.

**Table 4-1:** Dry solids cake formed of MFT flocculation using Chito-CTA of varying CTA/chitosan molar ratios and dosages, and Chito-g-PAM.

<b>Compound</b>	<b>Weight %</b>
<b>Chito-CTA (165)</b>	9.78
<b>Chito-CTA (326)</b>	11.12
<b>Chito-CTA (652)</b>	15.96
<b>Chito-CTA (978)</b>	20.32
<b>Chito-CTA (1304)</b>	23.86
<b>Chito-g-PAM</b>	25.43

Figure 4-6.A shows the SRF of MFT after treatment with Chito-CTA of varying CTA/chitosan molar ratios and dosages. As we increased the dosage of Chito-CTA, SRF dropped to a minimum of  $3.80 \cdot 10^{12}$  m/kg using 7000 or 10000 ppm of Chito-CTA (CTA/Chitosan = 1304). At higher dosages, Chito-CTA forms more compact flocs that expel water more easily.

Figure 4-6.B compares the SRF for Chito-CTA (CTA/chitosan = 1304), Chito-g-PAM, and C-PAM. Both chitosan-based flocculants produced sediments with significantly lower SRF values than the commercial C-PAM flocculant. Although Chito-CTA may become polar due to the quaternary modification with CTA, the incomplete deacetylation makes it partially hydrophobic, causing the MFT flocs to expel water more easily.

Chito-g-PAM and Chito-CTA produced sediments with similar SRF values, except when the dosage was 3000 ppm. The overall higher SRF of C-PAM likely arose from C-PAM's ability to hold significant amounts of water in the flocs. Chito-CTA and Chito-g-PAM, therefore, offer good alternatives for post flocculation treatment processes that involve filtration at moderate pressures to recover water and densify the sediments.

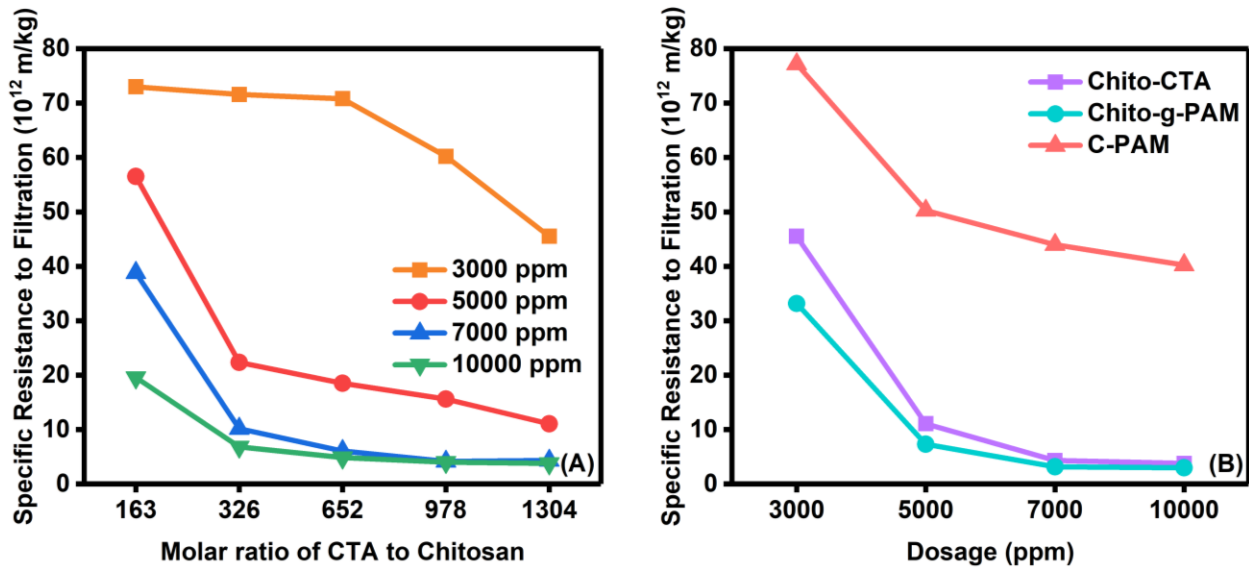


**Figure 4-6:** Specific resistance to filtration of MFT after the treatment using: (A) Chito-CTA of varying CTA/chitosan molar ratios and dosages, and (B) different dosages of Chito-CTA (CTA/chitosan = 1304), Chito-g-PAM, and C-PAM.

#### 4.6 Floc Formation in MFT

Figure 4-7.A shows the real-time evolution of floc size in MFT using 10000 ppm of Chito-CTA, Chito-g-PAM, and C-PAM (CTA/chitosan = 1304) measured by FBRM. Figure 4-7.A also provides information about the highest average floc size, change of average floc size over time, floc stability, and the time required to induce floc formation.

The commercial C-PAM formed flocs with largest sizes ( $32 \mu\text{m}$ ), but floc size decreased significantly over time. On the other hand, flocs formed using Chito-CTA and Chito-g-PAM grew up to maximum of  $25 \mu\text{m}$ , but their average sizes did not change appreciably over the flocculation period. Flocs formed using C-PAM were not very stable, perhaps because the flocs broke due to inefficient/weak adsorption of C-PAM onto the MFT clay surfaces. Contrarily, flocs formed with Chito-CTA and Chito-g-PAM reached stable sizes after approximately 300 s.

The time required for the adsorption of polymer chains onto particles, and subsequent floc formation, is called *characteristic adsorption time*. It is defined as

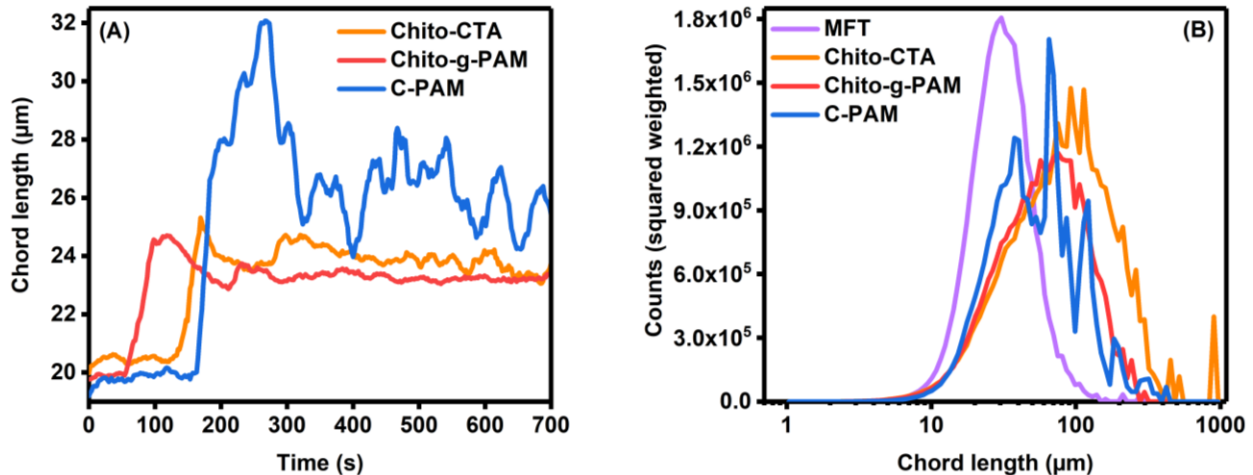
$$t_{ads} = \frac{-\ln(1 - f)}{k N} \quad (4.1)$$

where,  $f$  is the fraction of polymer needed to adsorb onto the clay surface and induce flocculation,  $k$  is the frequency of collisions between polymer molecules and clay particles per unit time, and  $N$  is the initial number of particles per unit volume in the suspension. It is evident from Figure 4-7.A that the characteristic adsorption time was the highest for C-PAM and the lowest for Chito-g-PAM. The graft microstructure of Chito-g-PAM possibly helped it adsorb onto the clay surfaces and form flocs faster than Chito-CTA and C-PAM.

Figure 4-7.B compares the floc size distribution when a dosage of 10000 ppm of Chito-CTA, Chito-g-PAM, and C-PAM was used. We used *square weighted* counts because it resolves even small changes in floc size [93–95].

The average of 10 particle size distributions (PSD) for pure MFT and for flocs produced with each flocculant are compared in Figure 4-7.B. Chito-CTA and Chito-g-PAM made flocs with smoother PSD than C-PAM, and the PSD for Chito-CTA is shifted to higher particles sizes, which agrees with the results in Figure 4-7.A, where the chord length of flocs made with Chito-CTA is higher than for Chito-g-PAM.

The PSD results for C-PAM, however, are less conclusive. Figure 4-7.A shows that the flocs with the highest chord lengths are formed with C-PAM. This result, however, contradicts the



PSD for C-PAM in Figure 4-7.B, which is very similar in range to that of flocs made with Chito-g-PAM. This apparent contradiction may be attributed to the noisier results obtained when C-PAM was used to flocculate MFT. It seems that C-PAM produced flocs that were unstable and fluctuated in size throughout the flocculation. We visually observed that C-PAM produced sludge/sediments with significantly large water entrainment that were likely shear-sensitive. Large flocs settle faster and may not be detected by the FPRM probe, while smaller flocs, resulting from the breakage of the weak larger flocs may be re-suspended and detected by the FBRM probe, causing the observed distortion in the PSD reported in Figure 4-7.B.

**Figure 4-7:** FBRM measurements for cord length and particle size distribution: (A) average floc size in MFT using 10000 ppm of Chito-CTA (CTA/chitosan = 1304), Chito-g-PAM, and C-PAM, (B) floc size distribution in MFT and MFT flocculated with 10000 ppm of Chito-CTA, Chito-g-PAM, and C-PAM

## 5 Conclusions and Future work

Two novel MFT flocculants were synthesized and tested in this thesis: chitosan modified with 3-chloro-2-hydroxypropyl trimethylammonium chloride (Chito-CTA) and chitosan grafted with polyacrylamide (Chito-g-PAM). We compared the flocculation performance of these two flocculants with a commercial cationic polyacrylamide (C-PAM) flocculant, because both Chito-CTA and Chito-g-PAM are also cationic polymers. CTA caused the quaternization of chitosan, increasing its solubility in water. The degree of quaternization was varied by changing the CTA/chitosan mole ratio from 163 to 1304. Free radical polymerization of acrylamide produced PAM grafts onto the chitosan backbone.

It is important to point out that no  $\text{Ca}^{2+}$  was added to help flocculation, which is desirable for recycling the water recovered from MFT flocculation.

Chito-g-PAM settled MFT faster than Chito-CTA, while C-PAM could not even form a distinct solid-liquid separation mudline.

Chito-g-PAM dewatered MFT quicker than Chito-CTA and C-PAM, as evidenced by CST measurements. It is conceivable that the hydrophobic chitosan backbones reduced the amount of water entrapped in the flocs, in comparison with the commercial high molecular weight C-PAM.

Among the three flocculants Chito-g-PAM exhibited a higher fraction of hydrophobicity that caused faster dewatering of MFT. Supernatant turbidity was significantly lower at all dosages tested for Chito-g-PAM. Chito-CTA and Chito-g-PAM offered similar specific resistance to filtration (SRF) at all dosages tested in this work.

Focused beam reflectance measurement (FBRM) enabled us to determine the highest average floc size, changes in average floc size over time, floc stability, and time required to induce floc formation. Chito-CTA and Chito-g-PAM produced flocs with a maximum cord length of 25  $\mu\text{m}$ , which were stable throughout the flocculation. C-PAM created flocs/sludge with uneven floc sizes that seemed to fluctuate during the flocculation. Chito-CTA produced flocs with a broad floc size distribution, showing its ability to capture particles with a wide range of sizes.

These chitosan-based flocculants seem to hold some promise to effectively dewater MFT, although further modifications are needed to make them commercially competitive. A few lines for future research are proposed below:

1. The length, density, and degree of hydrolysis of the PAM grafts was not investigated in this thesis. It is likely that this variable will have a significant effect in the flocculation performance of Chito-g-PAM. An optimization study for these variables could substantially increase the performance of Chito-g-PAM flocculants.
2. The current investigation only considered PAM grafts, but other graft types could be added to the Chito-CTA template. For instance, cationic monomers such as dimethyl acryloyloxyethyl benzyl ammoniumchloride could generate grafts that would increase the cationic charge and molecular weight of the flocculant, and also make the grafts moderately hydrophobic, which may trap less water in the flocs.
3. Chitosan has amino and hydroxyl groups that can be used during chemical modifications of its backbone. Hydrophilic groups can be added to the structure such as hydroxypropyl, dihydroxyethyl, hydroxyalkylamino, sulfate, phosphate, and

carboxymethyl grating agents. They will increase the solubility of chitosan in water adding charges to the structure. These new “chitosan templates” may be more effective backbones for the generation of grafted flocculants than the Chito-CTA used herein.

## 6 References

- [1] GEA, 2012: Global Energy Assessment - Toward a Sustainable Future, International Institute for Applied Systems Analysis, Vienna, Austria and Cambridge University Press, Cambridge, UK and New York, NY, USA, 2012.
- [2] J. Hanania, K. Stenhouse, J. Donev, Oil sands tailings ponds - Energy Education. [http://energyeducation.ca/encyclopedia/Oil\\_sands\\_tailings\\_ponds](http://energyeducation.ca/encyclopedia/Oil_sands_tailings_ponds) (accessed November 20, 2017).
- [3] M. Mech, A comprehensive guide to the alberta oil sands understanding the environmental and human impacts, export implications, and political, economic, and industry influences, 2011.
- [4] J. Rodríguez-Estival, J.E.G. Smits, Small mammals as sentinels of oil sands related contaminants and health effects in northeastern Alberta, Canada, *Ecotoxicol. Environ. Saf.* 124 (2016) 285–295.
- [5] M. Sherval, Canada’s oil sands: The mark of a new “oil age” or a potential threat to Arctic security?, *Extr. Ind. Soc.* 2 (2015) 225–236.
- [6] M. Humphries, North American Oil Sands: History of Development, Prospects for the Future, United States Congressional Research Service, 2012.
- [7] Government of Alberta, Facts and Statistics, (2007).  
<http://www.energy.alberta.ca/OilSands/791.asp> (accessed November 1, 2017).
- [8] C. Li, L. Fu, J. Stafford, M. Belosevic, M.G. El-Din, The toxicity of oil sands process-affected water (OSPW): A critical review, *Sci. Total Environ.* 601-602 (2016) 1785-1802.
- [9] Alberta Energy Regulator, Crude Bitumen Demand, Upgraded and nonupgraded bitumen. <https://www.aer.ca/data-and-publications/statistical-reports/crude-bitumen-demand> (accessed November 1, 2017).
- [10] W.R. Freudenberg, A Life in Social Research, vol:21, Emerald Group Publishing Limited, Bingley, 2013.

- [11] Y. Lu, Y. Shang, X. Huang, A. Chen, Z. Yang, Y. Jiang, J. Cai, W. Gu, X. Qian, H. Yang, R. Cheng, Preparation of Strong Cationic Chitosan-*graft*-Polyacrylamide Flocculants and Their Flocculating Properties, *Ind. Eng. Chem. Res.* 50 (2011) 7141–7149.
- [12] C.E.V. Collins, J.M. Foght, T. Siddique, Co-occurrence of methanogenesis and N<sub>2</sub> fixation in oil sands tailings, *Sci Total Environ.* 565 (2016) 306-312.
- [13] Q. Lu, B. Yan, L. Xie, J. Huang, Y. Liu, H. Zeng, A two-step flocculation process on oil sands tailings treatment using oppositely charged polymer flocculants, *Sci. Total Environ.* 565 (2016) 369–375.
- [14] BGC Engineering Inc., 2010. Oil Sands Tailings Technology Review. Oil Sands Research and Information Network, University of Alberta, School of Energy and the Environment, Edmonton, Alberta. OSRIN Report No. TR-1. 136 pp.
- [15] C.C. Small, S. Cho, Z. Hashisho, A.C. Ulrich, Emissions from oil sands tailings ponds: Review of tailings pond parameters and emission estimates, *J. Pet. Sci. Eng.* 127 (2015) 490–601.
- [16] Oil sands fever series, What is the highest environmental impact oil? <https://www.pembina.org/reports/mining-vs-in-situ.pdf> (accessed November 27, 2017).
- [17] A.T. Lima, K. Mitchell, D.W. O’Connell, J. Verhoeven, P.V. Cappellen, The legacy of surface mining: Remediation, restoration, reclamation and rehabilitation, *Environ. Sci. Policy.* 66 (2016) 227–233.
- [18] Oil Sands Magazine, Water Usage.  
<http://www.oilsandsmagazine.com/technical/environment/water-usage> (accessed November 27, 2017).
- [19] Oil Sands Magazine, In-Situ Bitumen Extraction,  
<http://www.oilsandsmagazine.com/technical/in-situ> (accessed November 27, 2017).
- [20] B. Ali, A. Kumar, Development of life cycle water footprints for oil sands-based transportation fuel production, *Energy.* 131 (2017) 41–49.
- [21] H.S. Niasar, H. Li, T.V.R. Kasanneni, M.B. Ray, C.C. Xu, Surface amination of activated

- carbon and petroleum coke for the removal of naphthenic acids and treatment of oil sands process-affected water (OSPW), *Chem. Eng. J.* 293 (2016) 189–199.
- [22] E.W. Allen, Process water treatment in Canada’s oil sands industry: I. Target pollutants and treatment objectives, *J. Environ. Eng. Sci.* 7 (2008) 123–138.
- [23] Oil Sands Tailings Consortium, Technical Guide for Fluid Fine Tailings Management, [http://www.cosia.ca/uploads/documents/id7/TechGuideFluidTailingsMgmt\\_Aug2012.pdf](http://www.cosia.ca/uploads/documents/id7/TechGuideFluidTailingsMgmt_Aug2012.pdf) (accessed November 1, 2017).
- [24] M. Li, S.L. Barbour, B.C. Si, Measuring Solid Percentage of Oil Sands Mature Fine Tailings Using the Dual Probe Heat Pulse Method, *J. Environ. Qual.* 44 (2015) 293.
- [25] S. Bourguès-Gastaud, P. Dolez, E. Blond, N. Touze-Foltz, Dewatering of oil sands tailings with an electrokinetic geocomposite, *Miner. Eng.* 100 (2017) 177–186.
- [26] Government of Canada, Oil Sands: Economic contributions, <http://www.nrcan.gc.ca/energy/publications/18756> (accessed November 1, 2017).
- [27] L.G. Reis, R.S. Oliveira, T.N. Palhares, L.S. Spinelli, E.F. Lucas, D.R.L. Vedoy, E. Asare, J.B.P. Soares, Using acrylamide/propylene oxide copolymers to dewater and densify mature fine tailings, *Miner. Eng.* 95 (2016) 29–39.
- [28] D.R.L. Vedoy, J.B.P. Soares, Water-soluble polymers for oil sands tailing treatment: A Review, *Can. J. Chem. Eng.* 93 (2015) 888–904.
- [29] R.J. Mikula, K.L. Kasperski, R.D. Burns, M.D. MacKinnon, Nature and fate of oil sands fine tailings, *Advances in Chemistry.* 251 (1996) 677–723.
- [30] Oil Sands Magazine, Tailings Ponds 101, <http://www.oilsandsmagazine.com/technical/mining/tailings-ponds> (accessed November 30, 2017).
- [31] P. Nechita, Applications of Chitosan in Wastewater Treatment, in Dr. Emad Shalaby (Ed.), *Biological Activities and Application of Marine Polysaccharides*, InTech, 2017.
- [32] L. Botha, J.B.P. Soares, The Influence of Tailings Composition on Flocculation, *Can. J. Chem. Eng.* 93 (2015) 1514–1523.

- [33] A.F. Demirörs, J.C.P. Stiefelhagen, T. Vissers, F. Smalenburg, M. Dijkstra, A. Imhof, A. Van Blaaderen, Long-ranged oppositely charged interactions for designing new types of colloidal clusters, *Phys. Rev. X.* 5 (2015).
- [34] R.J. Chalaturnyk, J. Don Scott, B. Özüm, Management of oil sands tailings, *Pet. Sci. Technol.* 20 (2002) 1025–1046.
- [35] R.Hogg, Flocculation and dewatering, *Int. J. Miner. Process.* 58 (2000) 223–236.
- [36] N.A. Oladoja, Headway on natural polymeric coagulants in water and wastewater treatment operations, *J. Water Process Eng.* 6 (2015) 174–192.
- [37] Y.J. Cui, F. Emeriault, F. Cui, S. Ghabezloo, J.M. Pereira, M. Reboul, H. Ravel, A.M. Tang, Proceedings of the 5th International Young Geotechnical Engineers' Conference, vol 2, Millpress, 2013.
- [38] R.K. Singhal, A.K. Mehrotra, Environmental issues and management of waste in energy and mineral production : proceedings of the Sixth International Symposium, CRC Press, Calgary, 2000.
- [39] S. Gosh, G. Sen, U. Jha, S. Pal, Novel biodegradable polymeric flocculant based on polyacrylamide-grafted tamarind kernel polysaccharide, *Bioresour. Technol.* 101 (2010) 9638–9644.
- [40] L. Ghimici, M. Nichifor, Novel biodegradable flocculating agents based on cationic amphiphilic polysaccharides, *Bioresour. Technol.* 101 (2010) 8549–8554.
- [41] F. Renault, B.Sancey, P.M. Badot, G.Crini, Chitosan for coagulation/flocculation processes – An eco-friendly approach, *Eur. Polym. J.* 45 (2009) 1337–1348.
- [42] Q. Chang, X. Hao, L. Duan, Synthesis of crosslinked starch-graft-polyacrylamide-co-sodium xanthate and its performances in wastewater treatment, *J. Hazard. Mater.* 159 (2008) 548–553.
- [43] Z. Yang, Y. Shang, Y. Lua, Y. Chen, X. Huang, A. Chen, Y. Jiang, W. Gu, X. Qian, H. Yang, R. Cheng, Flocculation properties of biodegradable amphoteric chitosan-based flocculants, *Chem. Eng. J.* 172 (2011) 287–295.

- [44] C.S. Lee, J. Robinson, M.F. Chong, A review on application of flocculants in wastewater treatment, *Process Saf. Environ. Prot.* 92 (2014) 489–508.
- [45] N. Yuan, L. Xu, L. Zhang, H. Ye, J. Zhao, Z. Liu, J. Rong, Superior hybrid hydrogels of polyacrylamide enhanced by bacterial cellulose nanofiber clusters, *Mater. Sci. Eng. C.* 67 (2016) 221–230.
- [46] Y. Wei, F. Cheng, H. Zheng, Synthesis and flocculating properties of cationic starch derivatives, *Carbohydr. Polym.* 74 (2008) 673–679.
- [47] K. Azlan, W.N.W. Saime, L.L. Ken, Chitosan and chemically modified chitosan beads for acid dyes sorption, *J. Environ. Sci.* 21 (2009) 296–302.
- [48] Y.D. Yan, S.M. Glover, G.J. Jameson, S. Biggs, The flocculation efficiency of polydisperse polymer flocculants, *Int. J. Miner. Process.* 73 (2004) 161–175.
- [49] K. Okaiyeto, U.U. Nwodo, S.A. Okoli, L. V. Mabinya, A.I. Okoh, Implications for public health demands alternatives to inorganic and synthetic flocculants: bioflocculants as important candidates, *Microbiologyopen.* 5 (2016) 177–211.
- [50] J.R.M. Kennedy, K.E. Kent, J.R. Brown, Rheology of dispersions of xanthan gum, locust bean gum and mixed biopolymer gel with silicon dioxide nanoparticles, *Mater. Sci. Eng. C.* 48 (2015) 347–353.
- [51] Z. Yang, H. Yang, Z. Jiang, T. Cai, H. Li, H. Li, A. Li, R. Cheng, Flocculation of both anionic and cationic dyes in aqueous solutions by the amphoteric grafting flocculant carboxymethyl chitosan-graft-polyacrylamide, *J. Hazard. Mater.* 254–255 (2013) 36–45.
- [52] D. Zhao, H. Liu, W. Guo, L. Qu, C. Li, Effect of inorganic cations on the rheological properties of polyacrylamide/xanthan gum solution, *J. Nat. Gas Sci. Eng.* 31 (2016) 283–292.
- [53] H. Salehizadeh, N. Yan, R. Farnood, Recent advances in polysaccharide bio-based flocculants, *Biotechnol. Adv.* (2017).
- [54] R. Yang, H. Li, M. Huang, H. Yang, A. Li, A review on chitosan-based flocculants and their applications in water treatment, *Water Res.* 95 (2016) 59–89.

- [55] R.G. Sharp, A review of the applications of chitin and its derivatives in agriculture to modify plant-microbial interactions and improve crop yields, *Agronomy*. 3 (2013) 757–793.
- [56] A.K. H.P.S, C.K. Saurabh, A. A.S., M.R. Nurul Fazita, M.I. Syakir, Y. Davoudpour, M. Rafatullah, C.K. Abdullah, M.K. M. Haafiz, R. Dungani, A review on chitosan-cellulose blends and nanocellulose reinforced chitosan biocomposites: Properties and their applications, *Carbohydr. Polym.* 150 (2016) 216–226.
- [57] M.N.V.R. Kumar, R.A.A. Muzzarelli, .C. Muzzarelli, H. Sashiwa, A.J. Dombl, Chitosan chemistry and pharmaceutical perspectives, *Chem. Rev.* 104 (2004). 6017–6084.
- [58] M.T. Yen, J.H. Yang, J.L. Mau, Physicochemical characterization of chitin and chitosan from crab shells, *Carbohydr. Polym.* 75 (2009) 15–21.
- [59] F. Croisier, C. Jérôme, Chitosan-based biomaterials for tissue engineering, *Eur. Polym. J.* 49 (2013) 780–792.
- [60] A. Jimtaisong, N. Saewan, Utilization of carboxymethyl chitosan in cosmetics, *Int. J. Cosmet. Sci.* 36 (2014) 12–21.
- [61] I. Younes, M. Rinaudo, Chitin and chitosan preparation from marine sources. Structure, properties and applications, *Mar. Drugs*. 13 (2015) 1133–74.
- [62] T. Furuike, D. Komoto, H. Hashimoto, H. Tamura, Preparation of chitosan hydrogel and its solubility in organic acids, *Int. J. Biol. Macromol.* 104 (2017) 1620–1625.
- [63] M.N. Gupta, S. Raghava, Smart systems based on polysaccharides, in: T.G. Volova, Y.S. Vinnik, E.I. Shishatskaya, N.M. Markelova, G.E. Zaikov (Eds.), *Natural-Based Polymers for Biomedical Applications*, Elsevier, 2008, pp. 129–161.
- [64] Y.J. Zheng, X.J. Loh, Natural rheological modifiers for personal care, *Polym. Adv. Technol.* 27 (2016) 1664–1679.
- [65] C.Y. Teh, P.M. Budiman, K.P.Y. Shak, T.Y. Wu, Recent advancement of coagulation–flocculation and its application in wastewater treatment, *Ind. Eng. Chem. Res.* 55 (2016) 4363–4389.
- [66] C.H. Leng, M.A.A. Razali, M.R.H. Rosdi, A. Ariffin, Composite flocculants based on

- magnesium salt–polydiallyldimethylammonium chloride: characterization and flocculation behaviour, *RSC Adv.* 5 (2015) 53462–53470.
- [67] M.M. Hassan, Binding of a quaternary ammonium polymer-grafted-chitosan onto a chemically modified wool fabric surface: assessment of mechanical, antibacterial and antifungal properties, *RSC Adv.* 5 (2015) 35497–35505.
- [68] C. Wan, M.A. Alam, X.Q. Zhao, X.Y. Zhang, S.L. Guo, S.H. Ho, J.S. Chang, F.W. Bai, Current progress and future prospect of microalgal biomass harvest using various flocculation technologies, *Bioresour. Technol.* 184 (2015) 251–257.
- [69] H. Tan, R. Ma, C. Lin, Z. Liu, T. Tang, Quaternized chitosan as an antimicrobial agent: antimicrobial activity, mechanism of action and biomedical applications in orthopedics, *Int. J. Mol. Sci.* 14 (2013) 1854–1869.
- [70] X.G. Chen, H.J. Park, Chemical characteristics of O-carboxymethyl chitosans related to the preparation conditions, *Carbohydr. Polym.* 53 (2003) 355–359.
- [71] S. Thomas, P.A. Soloman, V.O. Rejini, Preparation of Chitosan- CMC Blends and Studies on Thermal Properties, *Procedia Technol.* 24 (2016) 721–726.
- [72] Z. Cai, Z. Song, S. Shang, C. Yang, Study on the flocculating properties of quaternized carboxymethyl chitosan, *Polym. Bull.* 59 (2007) 655–665.
- [73] R.O. Pedro. C.C. Schmitt, M.G. Neumann, Syntheses and characterization of amphiphilic quaternary ammonium chitosan derivatives, *Carbohydr. Polym.* 147 (2016) 97–103.
- [74] M. He, C.-C. Chu, Dual stimuli responsive glycidyl methacrylate chitosan-quaternary ammonium hybrid hydrogel and its bovine serum albumin release, *J. Appl. Polym. Sci.* 130 (2013) 3736–3745.
- [75] A.L. Bukzem, R. Signini, D.M. dos Santos, L.M. Lião, D.P.R. Ascheri, Optimization of carboxymethyl chitosan synthesis using response surface methodology and desirability function, *Int. J. Biol. Macromol.* 85 (2016) 615-624.
- [76] S. Tseng, Y.R. Hsu, J.P. Hsu, Diffusiophoresis of polyelectrolytes: Effects of temperature, pH, type of ionic species and bulk concentration, *J. Colloid Interface Sci.* 459 (2015) 167–

174.

- [77] K.E. Lee, T.T. Teng, N. Morad, B.T. Poh, M. Mahalingam, Flocculation activity of novel ferric chloride–polyacrylamide (FeCl<sub>3</sub>-PAM) hybrid polymer, *Desalination*. 266 (2011) 108–113.
- [78] J. Zhang, Y. Yuan, J. Shen, S. Lin, Synthesis and characterization of chitosan grafted poly(N,N-dimethyl-N-methacryloxyethyl-N-(3-sulfopropyl) ammonium) initiated by ceric (IV) ion, *Eur. Polym. J.* 39 (2003) 847–850.
- [79] J.M. Joshi, V.K. Sinha, Ceric ammonium nitrate induced grafting of polyacrylamide onto carboxymethyl chitosan, *Carbohydr. Polym.* 67 (2007) 427–435.
- [80] R. Bhargava, S.Q. Wang, J.L. Koenig, FTIR microspectroscopy of polymeric systems, in *Liquid Chromatography / FTIR Microspectroscopy / Microwave Assisted Synthesis*, Springer, Berlin, 2003, pp. 137–191.
- [81] M.A. Mohamed, J. Jaafar, A.F. Ismail, M.H.D. Othman, M.A. Rahman, Fourier Transform Infrared (FTIR) Spectroscopy, in: *Membr. Charact.*, Elsevier, 2017: pp. 3–29.
- [82] J.L. Koenig, *Spectroscopy of polymers*, second ed., Elsevier, Oxford, 1999.
- [83] M.K. Mishra, *Handbook of encapsulation and controlled release*, first ed., CRC Press, Boca Raton, 2015.
- [84] D.K. Thompson, F.L. Motta, J.B.P. Soares, Investigation on the flocculation of oil sands mature fine tailings with alkoxysilanes, *Miner. Eng.* 111 (2017) 90–99.
- [85] R. Das S. Ghorai, S. Pal, Flocculation characteristics of polyacrylamide grafted hydroxypropyl methyl cellulose: An efficient biodegradable flocculant, *Chem. Eng. J.* 229 (2013) 144–152.
- [86] M. Scholz, Review of recent trends in capillary suction time (CST) dewaterability testing research, *Ind. Eng. Chem. Res.* 44 (2005) 8157–8163.
- [87] O. Sawalha, M. Scholz, Assessment of capillary suction time (CST) test methodologies, *Environ. Technol.* 28 (2007) 1377–1386.
- [88] Y. Xua, T. Dabrosa, J. Kanb, Filterability of oil sands tailings, *Process Saf. Environ. Prot.*

86 (2008) 268–276.

- [89] S.P. Gumfekar, T.R. Rooney, R.A. Hutchinson, J.B.P. Soares, Dewatering oil sands tailings with degradable polymer flocculants, *ACS Appl. Mater. Interfaces*. 9 (2017) 36290–36300.
- [90] C. Wang, C. Han, Z. Lin, J. Masliyeh, Q. Liu, Z. Xu, Role of preconditioning cationic zetag flocculant in enhancing mature fine tailings flocculation, *Energy & Fuels*. 30 (2016) 5223–5231.
- [91] C. Klein, D. Harbottle, L. Alagha, Z. Xu, Impact of fugitive bitumen on polymer-based flocculation of mature fine tailings, *Can. J. Chem. Eng.* 91 (2013) 1427–1432.
- [92] D. Zhang, T. Thundat, R. Narain, Flocculation and dewatering of mature fine tailings using temperature-responsive cationic polymers, *Langmuir*. 33 (2017) 5900–5909.
- [93] A.R. Heath, P.D. Fawell, P.A. Bahri, J.D. Swift, Estimating average particle size by focused beam reflectance measurement (FBRM), *Part. Part. Syst. Charact.* 19 (2002) 84–95.
- [94] A.F.Grabsch, P.D. Fawell, S.J. Adkins, A. Beveridge, The impact of achieving a higher aggregate density on polymer-bridging flocculation, *Int. J. Miner. Process.* 124 (2013) 83–94.
- [95] L. Botha, S. Davey, B. Nguyen, A.K. Swarnakar, E. Rivard, J.B.P. Soares, Flocculation of oil sands tailings by hyperbranched functionalized polyethylenes (HBfPE), *Miner. Eng.* 108 (2017) 71–82.